Resolving urban mobility networks from individual travel graphs using massive-scale mobile phone tracking data

Jinzhou Cao[1,2], Qingquan Li [1, 2,3], Wei Tu[1,2*], Qili Gao[1,2], Rui Cao[1,2], Chen Zhong[4]

[1] Guangdong Key Laboratory of Urban Informatics, Shenzhen Key Laboratory of Spatial Smart Sensing & Research Institute of Smart Cities, Shenzhen University, Shenzhen 518060, China

[2] Department of Urban Informatics, School of Architecture and Urban Planning, Shenzhen University, Shenzhen 518060, China

[3] State Key Laboratory of Information Engineering in Surveying, Mapping, and Remote Sensing, Wuhan University, Wuhan 430079, China

[4] Department of Geography, King's College London, London WC2R 2LS, UK

Corresponding author: Dr. Wei Tu

Email: tuwei@szu.edu.cn

Address: Kejilou 1402, Shenzhen University

Nanhai road No. 3688, Shenzhen 430079, P. R. China

Acknowledgments

The authors would like to thank all colleagues and students who contributed to this study. This research was jointly supported by the Natural Science Foundation of China [42001393 and 71961137003]; the China Postdoctoral Science Foundation [2020M672803]; the Natural Science Foundation of Guangdong Provinces [2019A1515011049]; the Basic Research Program of Shenzhen Science and Technology Innovation Committee [JCJY20180305312511383], and the Open Fund of Key Laboratory of Urban Land Resources Monitoring and Simulation Ministry of Natural Resources[KF-2019-04-073].

Abstract

Human movements and interactions with cities are characterized by urban mobility networks. Many studies that address urban mobility are inspired by complex networks. The models of complex networks require a large amount of empirical data. However, current works relied on traditional survey data and were unable to take full advantage of the capabilities offered by complex networks; thus, the possibility of quantifying urban mobility networks by considering individual travel patterns has not yet been addressed. This study presents a data-driven approach for characterizing urban mobility networks based on massive-scale mobile phone tracking data. Individual travel motifs are first extracted using a graph-based approach. The global urban mobility network (*G-UMN*) and the motif-dependent urban mobility subnetworks (*MD-UMN*s) are then constructed. Next, network properties, including statistical measures and scaling relations between the basic measures, are proposed for characterizing mobility networks. We have conducted experiments focusing on Shenzhen, China. The results demonstrated that (1) the individual travel motifs are structurally and spatially heterogeneous, (2) the *G-UMN* exhibits a evolutionary hierarchical structure, and (3) the *MD-UMN*s show many behavioral differences in their spatial and topological properties, reflecting the impacts of the heterogeneity of the individual travel motifs. These results bridge the gap between complex network properties and urban mobility patterns and provide crucial implications and policies for data-informed urban planning.

Key Words: Spatial network; Urban mobility; Mobile phone tracking data; Complex Network analysis.

1 Introduction

Rapid urbanization has led to a great influx of residents into cities. The intra-urban movements of individuals are rapidly changing. Moreover, frequent human movements and the associated interactions with urban space pose great challenges to urban planning by demanding an urban spatial structure that is compatible with highly efficient travel for residents. Urban mobility is crucial for harmonizing urban spatial structures since it exerts significant influences on resource allocation, social equity and sustainable urban evolution (Maeda et al., 2019; Toole et al., 2015). Consequently, the ability to characterize urban mobility attracts scholarly attention in a broad range of fields, from urban planning (Ratti et al., 2006), transport (Tu et al., 2019), and urban science (Batty, 2008) to statistical physics (Bettencourt, 2013).

How to characterize urban mobility has been intensively investigated recently. However, the representation of human movements is difficult. Since an individual's trajectory can be modeled as a graph, an innovative notion that is referred to as the 'urban mobility network' has been acknowledged as an effective foundation for urban mobility studies. The urban mobility network is defined as the network-oriented aggregation of individuals' movements in urban environments (Parthasarathi, 2014). Studies that characterize urban mobility networks have been employed to reveal the properties of urban mobility (Barthélemy, 2011; Cheng et al., 2013). Recently, several studies that address urban mobility are inspired by complex networks. Complex networks theory provides models to describe the topological and spatial patterns of networks. The statistics of mobility networks can thus describe and evaluate how human mobility is distributed and developed on different scales. Therefore, these complex network-driven measures have highlighted the characteristics of urban mobility (Agryzkov et al., 2017; Zhang & Thill, 2017). The models of complex networks require a large amount of empirical data. However, current works relied on traditional survey data and were unable to take full advantage of the capabilities offered by complex networks for addressing urban mobility tasks.

With technological advances in the fields of global positioning systems (GPS) and information and communications technology (ICT), ubiquitous smart devices have become sensors that individuals carry every day (Calabrese et al., 2014). These advances have contributed to an explosive growth of human tracking datasets, such as mobile phone positioning data (Alexander et al., 2015; Blondel et al., 2015) and GPS trajectories (Tang et al., 2015; Tu et al., 2018). These emerging datasets enable the high-precision representation of human movements (Shaw et al., 2016; Zhao et al., 2018) and create new windows for understanding human-urban interaction (Lim et al., 2018; Y. Wang et al., 2019; Xu et al., 2019). Thus, interpretable quantitative analyses of urban mobility networks are becoming possible. Some studies quantified urban mobility networks by aggregating the movements of all individuals(Hamedmoghadam et al., 2019; Louail et al., 2015; Riascos & Mateos, 2020). However, few studies simultaneously considered the heterogeneity of individual travels.

The properties of urban mobility networks are influenced by individual travel (Pinho et al., 2016; Puura et al., 2018). Because individual travel is shaped by personal characteristics and the spatial configurations of facilities, urban mobility shows various patterns (Zhang et al., 2018). Multifaceted urban mobility networks can be constructed to capture the corresponding characteristics. Therefore, this study addresses the following question: what are the heterogeneous properties of individual travels extracted from massive human tracking data? Furthermore, when aggregating individual travel into multifaceted urban mobility networks, another question is raised: what are the differences in the complex network properties of multifaceted urban mobility? These two questions highlight the necessity of a comprehensive and comparative study to investigate urban mobility networks using big human tracking data. We present a data-driven approach for resolving urban mobility networks. Individual trajectories are abstracted into standard graph-based motifs. The global urban mobility network is constructed by aggregating the travel graphs of all individuals, and multiple urban mobility subnetworks are constructed in accordance with the individual motifs; then, the resulting networks are characterized by a series of statistical measures derived from the complex network perspective. These measures allow us to reveal the patterns present in urban mobility networks. We also consider scaling relations between these measures to evaluate how urban mobility networks develop. Considering Shenzhen, China as the study area, we exploited massive-scale mobile phone tracking data to construct travel motifs of all individuals and characterized the urban mobility networks. The results of the statistical measures and scaling relations demonstrated a multi-facet portrait of urban mobility networks, which provides crucial implications and policies for data-informed urban planning.

This study makes the following contributions. First, compared with traditional approaches, this study resolves urban mobility networks by considering the impacts of the heterogeneity of individual travels using mobile phone tracking data, which have higher penetration and a finer temporal scale. Second, the results of this study provide a deeper understanding of the structurally and spatially heterogeneous patterns of urban mobility networks. These insights thus help policy-makers to evaluate their urban development strategy, especially the urban resources allocation. Last, the findings of this study are complementary to urban studies in a different but typical urban context in the light of urban development path.

The remainder of this article is organized as follows. Section 2 reviews related works of this research. Section 3 introduces the study area and the mobile phone tracking data that are utilized. Section 4 describes the proposed methodological framework of resolving the urban mobility networks. Section 5 analyzes the results. Section 6 concludes the findings and policy suggestions and discusses future work.

2 Literature review

Urban mobility analysis is a fundamental research topic in interdisciplinary field which focuses on exploring the spatio-temporal properties as well as hidden patterns behind the intra-urban and inter-urban movements (González et al., 2008; Tu et al., 2018). The concept of urban mobility is broad in dimensions of human travels at both individual and group levels. The conceptualization of urban mobility also varies depending on the contexts of the range of applications, e.g., epidemic prevention(Gómez et al., 2018), migratory flows prediction(Huang et al., 2018), urban planning(Bokányi et al., 2019), and location-based services(Noulas et al., 2012).

The representation and characterization of urban mobility are the primary work in the urban mobility analysis(Hasan et al., 2012). In transportation planning and modeling, intra-urban human movements can be captured in the form of origin–destination (OD) matrices, where these matrices were obtained by dividing an area into a set of zones and counting the numbers of trips between two zones (Calabrese et al., 2011; Bachir et al., 2019). As a another example, inter-urban population migration can be described as a flow network by establishing the adjacency relationships of the population flows between two cities (Pan & Lai, 2019). These studies mark underlying efforts to model the structural form of urban mobility.

Since the intra-urban or inter-urban mobility can both modeled as a graph, the notion of ‘urban mobility network’ has been viewed as an important concept for urban mobility studies. Namely, it denotes the network-structured aggregation of population’s urban travels and activities(Parthasarathi, 2014). Recent years have witnessed explosive growth of big human mobility data in urban scenarios due to the advancements in the information and communications technology and pervasive usage of smart devices. Multi-sourced and massive data provide an unprecedented opportunity for a deeper understanding of urban mobility networks. Previous studies have been employed to derive urban mobility networks from human mobility data(Belyi et al., 2017). Topics include, but are not limited to, community-based spatial structures (Gao et al., 2013; Ratti et al., 2010; Yildirimoglu & Kim, 2017), intra-urban interactions (Krings et al., 2009; Sun et al., 2015; Wu et al., 2014; Zhang et al., 2017), traffic flow dynamics (Jiang et al., 2009; Liu et al., 2012; Tang et al., 2015), scaling laws of mobility (Brockmann et al., 2006; Tachet et al., 2017; Yan et al., 2013), and inter-urban migration patterns (De Montis et al., 2005; Liu et al., 2014; Simini et al., 2012). These studies highlighted the characterizations of urban mobility networks to better understand the human behaviors and the structures of cities.

Recently, several studies that mark urban mobility networks are motivated by complex network theory(Guidotti et al., 2016). A system consisting of several non-identical elements connected by diverse interactions is considered as a complex network where the nodes are the system elements and the links are the interactions between the elements(Newman, 2010). Complex networks theory develops various quantitative measures, such as the node degree, node strength, and clustering coefficient, to characterize one network(Albert & Barabási, 2002). Important properties in complex networks, such as the small-world properties(Watts & Strogatz, 1998), scale-free properties(Barabási & Albert, 1999) and community structures(Wang et al., 2018), have also been found in the urban mobility networks, and some studies have explained the dynamic mechanism of urban mobility behind these properties(Barabási, 2005; Lera et al., 2017). For instance, Saberi, et al. (2016) explored travel demand patterns by analyzing the measures of OD networks, including the node degree, node flux, and shortest path, using household travel survey data from Chicago and Melbourne. Zhong, et al. (2014) revealed urban spatial structures by examining the centralities of an urban network using travel survey data from Singapore. In recent years, big data have played a vital role in curving the urban mobility patterns through the complex network tools. For example, Chi, et al. (2016) and Hossmann, et al. (2011) applied complex network-driven measures to investigate mobility patterns by fusing social media check-ins, GPS trajectories, and smart card data. Louail et al. (2015) revealed the spatial structure of commuting networks extracted from mobile phone data. Although these studies revealed the overall look of urban mobility networks by aggregating the movements of large populations, there seem to be lack of the simultaneously consideration of the heterogeneity of individual travels. In other words, whether there exist any differences in properties of multifaceted urban mobility networks across various population classes remains to be better explored.

The scaling laws is seen as very effective to obtain a qualitative description of global character in urban mobility analysis. The scaling properties is proved to be widespread in urban mobility(Song, Koren, et al., 2010; X.-W. Wang et al., 2014). For example, power-law-like displacement distribution(Yan et al., 2013) and visitation frequency distribution(Zheng & Zhou, 2017) were empirically observed in many analyses of human movements. However, there is still a remarkable lack of research that would reveal the scaling relation between various complex network-based measures. With the increasing availability of human mobility datasets and the innovation in complex network methods, this paper therefore presents a complex network-based measure framework to characterize urban mobility networks from mobile phone tracking data, and further assess the development of mobility networks in a policy-oriented perspective.

3 Study area and data

3.1 Case study: Shenzhen, China

This study was conducted in Shenzhen, China, which is located in southern China and borders Hong Kong to the south, with a total area of approximately 2,050 square kilometers. The spatial map of Shenzhen is shown in Fig. 1. Shenzhen is a typical high-density city in the world. By the end of 2015, the residential population of Shenzhen was approximately 11 million and the population density of Shenzhen had reached 5,500 per square kilometer; it ranks first in China according to national statistics (Shenzhen Municipal Statistics Bureau, 2016).

Fig. 1. Study area of Shenzhen, China.

As the first Special Economic Zone (SEZ) in China, Shenzhen has experienced rapid urbanization. Over the past forty years, Shenzhen has transformed from a small fishing village into a prominent high-tech and innovative mega-city in China. In accordance with this governmental policy, Shenzhen was divided into an SEZ and a non-SEZ during the early years. The original SEZ districts included Luohu, Futian, Nanshan and Yantian districts, which are located in southern Shenzhen. The original non-SEZ districts included Bao'an, Longhua, Longgang, Pingshan, and Dapeng districts, which are located in northern and eastern Shenzhen. The SEZ and non-SEZ districts exhibited considerable differences in their urban and transport planning, and policies, which generated enormous gaps in their economic and social development. The SEZ districts have more accessible transport systems (buses and metros) , high-income job opportunities and abundant living resources, such as shopping malls, schools and universities, medical facilities, community parks. The non-SEZ districts contained many industrial parks and natural lands. In 2010, the SEZ was expanded to include the whole city; thus, an increasing number of urban resources were allocated to the original non-SEZ districts. However, these spatial differences in urban development still exist. For example, several SEZ districts have local centers that attract huge travels from neighboring districts while the other districts lacked business and cultural centers and resulted in many cross-regional travels. This situation emphasizes the necessity of resolving urban mobility and contributing to urban planning policies, such as how to narrow the regional differences of the city in the future.

3.2 Mobile phone tracking data

The mobile phone tracking data were utilized to construct individual. The dataset employed in this study were provided by a dominant communications operator in Shenzhen collected on a working day in March 2012. Unlike the data drawn from call detail records (CDRs), which are triggered only upon receipt of communication events (such as phone calls and text messages) (Xu et al., 2016; Yang, Fang, Yin, et al., 2019), the data applied in this study were recorded every hour. The corresponding service areas were approximated by Voronoi tessellation of base towers. The locations of the mobile phone users were determined at the base tower level. Therefore, this dataset shows advantages over CDRs and other traditional travel survey datasets in terms of its higher penetration rate and temporal resolution. To protect user privacy, this dataset has been anonymized by the communication operator. No personal information, such as phone number, username, gender, or age, can be obtained from the data. Examples of records of a user are presented in Table 1. One record includes a user ID, a timestamp, and latitude and longitude coordinates. There are approximately 9.7 million mobile phone users in one day. A total of 5,926 base towers exist in the study area.

Table 1. Examples of mobile phone tracking data

User ID	Longitude	Latitude	Time (hh: mm: ss)
1101032***	113.934***	22.521***	07: 25: 00
1101032***	113.882***	22.571***	08: 35: 00
1101032***	113.882***	22.571***	09: 26: 00
1101032***	113.882***	22.571***	10: 31: 00
…	…	…	…
1101032***	113.934***	22.521***	23: 28: 00

4 Methodology

An overarching framework has been developed to resolve urban mobility networks extracted from massive-scale mobile phone tracking data. This framework consists of three stages. The first stage abstracts individuals' travels into motifs by processing the raw mobile phone tracking data. The second stage produces the global urban mobility network and motif-dependent urban mobility subnetworks using abstracted individual motifs. The final stage examines the statistical measures of the mobility networks and the scaling relations of these measures to characterize urban mobility. Fig. 2 illustrates the workflow of the proposed analytical framework.

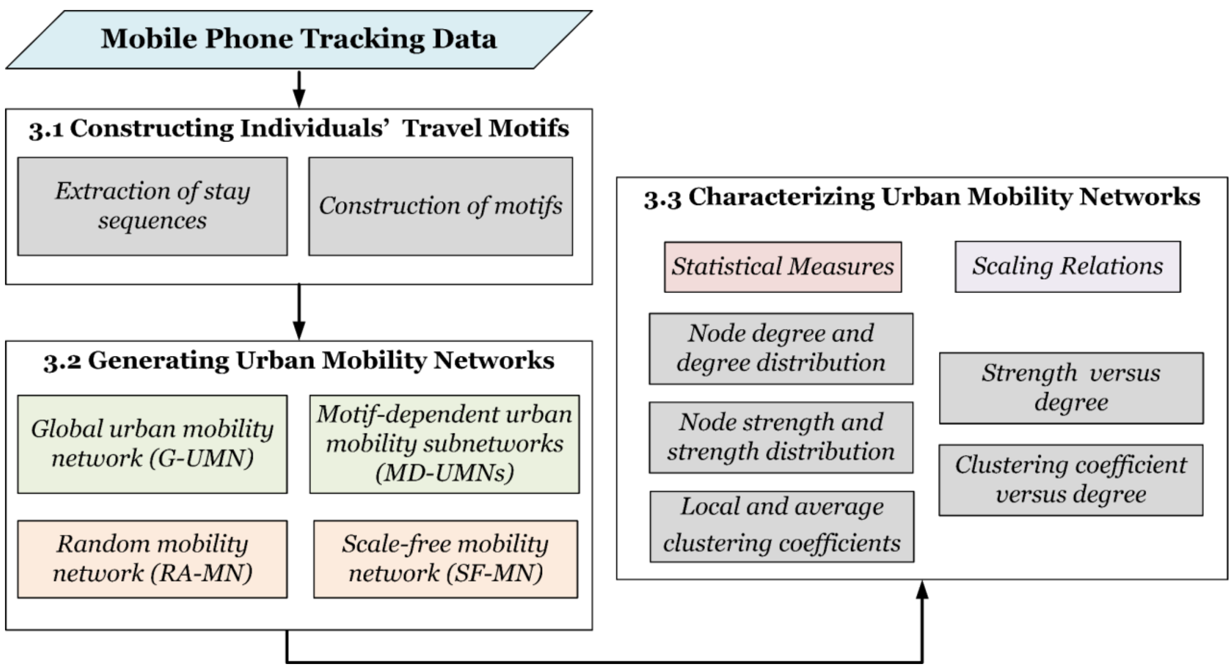

Fig. 2. Workflow of the proposed analytical framework.

4.1 Constructing individuals' travel motifs

By leveraging mobile phone tracking data, individual trajectories were abstracted into travel motifs using a two-step method. As illustrated in Fig. 3, the raw mobile phone tracking data were first segmented into sequential stays. Each stay sequence was then utilized to abstract a graph-based travel structure, which is referred to as a motif, in which each node denotes a distinct visited place and each edge denotes the travel flow between two places.

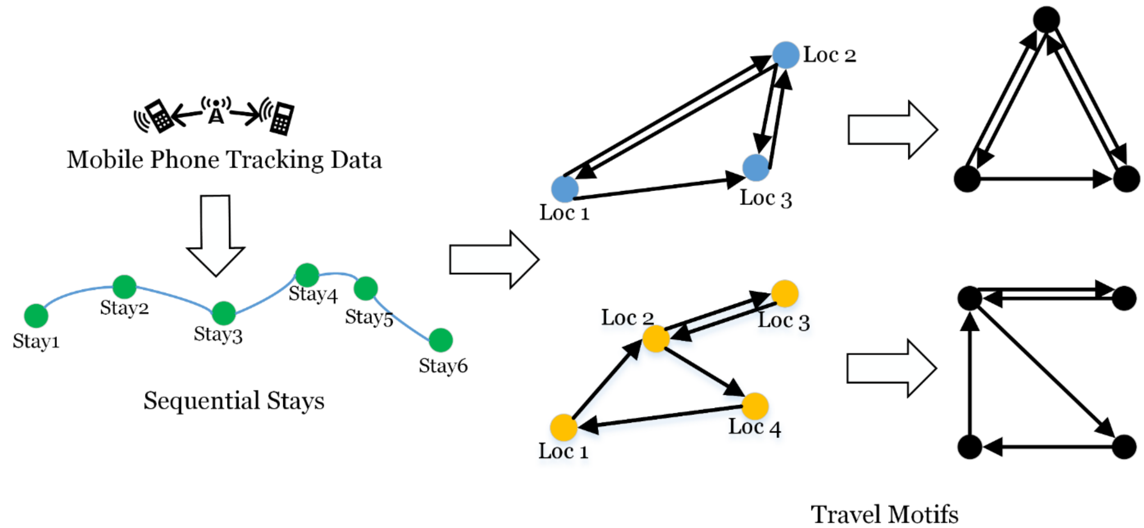

Fig. 3. The construction of individuals' travel motifs from mobile phone tracking records.

4.1.1 Extracting stay sequences

The records were sorted by the timestamp and clipped into time-sequential positioning records, as illustrated by the consecutive purple triquetrous points in Fig. 4. Here, sequential stays represent a set of places where users were engaged in activities (Shen & Cheng, 2016). We applied a tower-based segmentation algorithm using both spatial rules and temporal rules (Tu et al., 2017). We connected the time-sequential records with no move into candidate stays. The red vertical lines in Fig. 4 represent the five candidate stays (*p2-p5*, *p7-p9, p10-p12, p13-p14, p15-p17*). Spatial uncertainty exists because of the low spatial accuracy of cell-tower-based location technology. Consecutive records might jump between adjacent cell towers. Therefore, we calculated the spatial radius between each record that is not in any candidate stay and every candidate stay; if the distance is less than the 500 meters, the record was added to the candidate stay. As shown in Fig. 4, record *p6* can be merged into candidate *Stay 2*. Otherwise, the point was recognized as a new candidate stay. Once all twenty-four records for a particular person were processed, the corresponding sequence of candidate stays was identified. For all candidate stays, if the temporal duration is less than 60 minutes or shorter, the stay was not considered as a true stay. The temporal duration of candidate stay *p13-p14* was 50 minutes; this candidate stay was omitted. The true stay sequence was identified, as illustrated by the yellow points in Fig. 4. Note that any user with only one stay in his/her sequence was excluded because he/she did not move throughout the whole day. These sequential stays were employed to construct a directed graph.

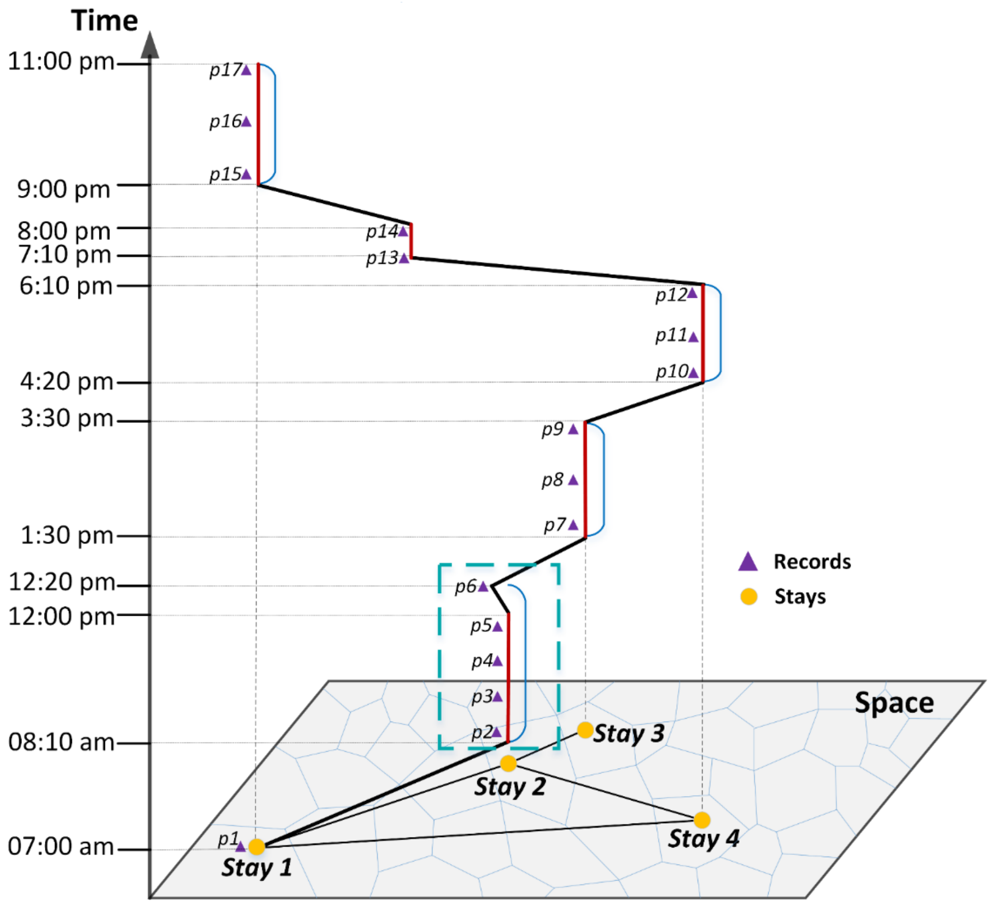

Fig. 4. Illustration of the extraction of stay sequences from mobile phone tracking data.

4.1.2 Constructing mobility motifs

Let M be the number of users eligible for analysis. Let the sequential stays of user u be denoted by $S(u) = \{Stay_1, Stay_2 \ldots, Stay_N\}$, where *N* is the number of separate visits to locations. Accordingly, the travel graph $G(u) = \{V(u), L(u)\}$ can be constructed from $S(u)$. The vertex set $V(u) = \{v_1, v_2, \cdots, v_n\}$ contains all distinct visited locations, where n is the number of distinct locations. The link set $L(u) = \{\ell_{i,j} | i, j \in V(u) \wedge i \neq j\}$ contains all directed trips, where $\ell_{i,j}$ is the directed flow between vertex i and vertex j. Essentially, $G(u)$ is expressed in weighted matrix form. Each individual's daily trips can be abstracted into a travel graph, which is referred to as a travel *motif,* where each node represents a distinct visited location and each edge represents the travel flow between a particular pair of nodes (Cao et al., 2019). Fig. 3 depicts the construction processes for motifs with three nodes (top) and four nodes (bottom). We applied the following convention to name the motifs (Fig. 5): *ID-2-1* represents the first motif with two nodes, *ID-3-1* represents the first motif with three nodes, etc.

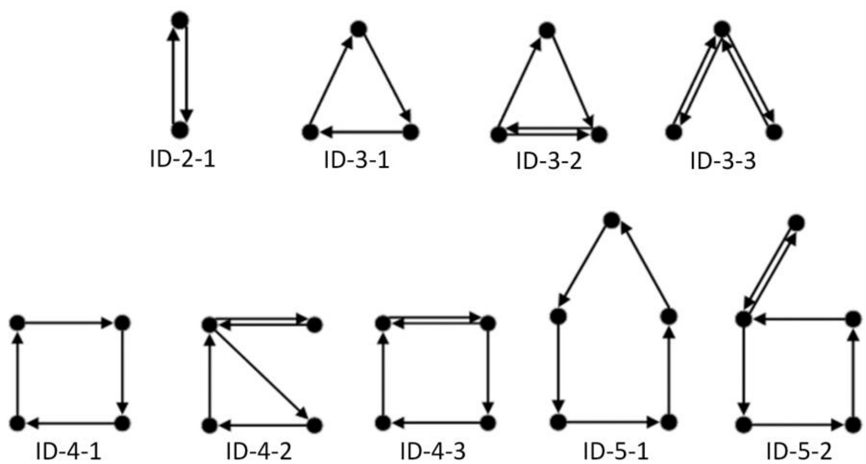

Fig. 5. Extracted most frequent motifs and their corresponding identities.

4.2 Generating urban mobility networks

The global urban mobility network was constructed by aggregating all individuals' travel motifs. Considering the different topologies of the motifs, multifaceted motif-dependent urban mobility subnetworks were also constructed. These subnetworks represent the heterogeneous characteristics of the individual travel patterns, as illustrated in Fig. 6. The random and scale-free urban mobility networks that represents two extreme urban mobility patterns were also generated as references.

4.2.1 Global urban mobility network

To capture a global picture of the urban mobility network, we aggregated all individuals' motifs to construct a weighted directed network that represented the sum of the travel flows of all individuals. We name this network the *global urban mobility network (G-UMN),* which is defined as

$$G_{G-UMN} = (V, E, W)$$

where $V = Distinct(\bigcup_{u=1}^{u=M} V(u))$ represents all of the distinct urban nodes (i.e., the service areas of the base towers) and $E = \{(v_i, v_j) | (v_i, v_j) \in distinct(\bigcup_{u=1}^{u=M} L(u))$ represents all existing flows between pairs of nodes. The edge weights $W_{v_i v_j}$ correspond to the counts of flows between two nodes. For each individual trip on edge (v_i, v_j), the weight $W_{v_i v_j}$ is incremented by 1. For each $(v_i, v_j) \in E$, we have $W(v_i, v_j) = W_{v_i v_j}$.

4.2.2 Motif-dependent urban mobility subnetworks

Multiple urban mobility subnetworks were constructed by using these travels with one type of individual motif. The data for all individuals that exhibit the same motif were aggregated into a corresponding weighted network. We refer to these networks as *motif-dependent urban mobility subnetworks (MD-UMNs)*. We applied the same identity convention that was applied to the motifs to express the identity of the subnetworks. The mathematical expression for an *MD-UMN is*

$$G_{MD-UMN}^{t} = (V^t, E^t, W^t)$$

where $V^t = Distinct(\bigcup_{u=1}^{u=P} V(u) \in V(t)\ in\ G_{Loc}(t))$ represents all of the urban nodes that belong to motif *t*, $E^t = \{(v_p, v_q)|(v_p, v_q) \in distinct(\bigcup_{u=1}^{u=P} E(u) \in E(t)\ in\ G_{Loc}(t))$ represents all flows that belong to motif *t*, and $\mathrm{W}^t(v_i, v_j)$ represents the absolute weight of edge (ℓ_i, ℓ_j) that belongs to motif *t*.

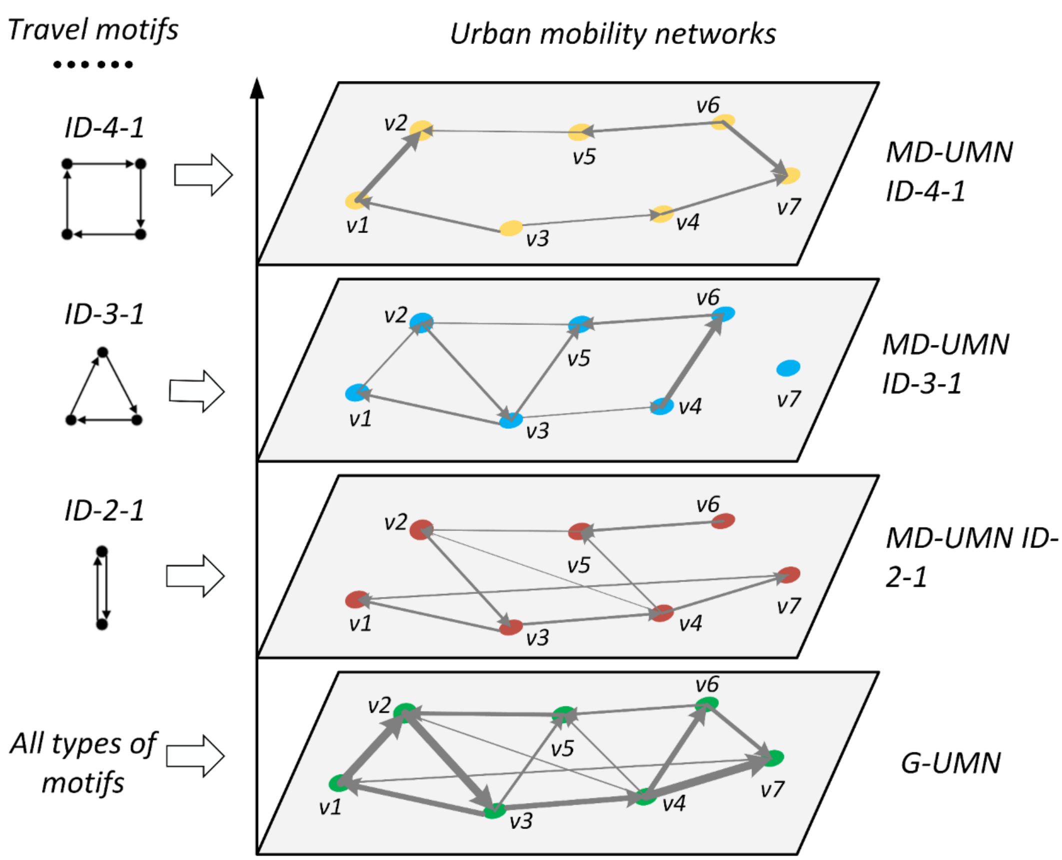

Fig. 6. Illustrations of the global urban mobility network *(G-UMN)* and the motif-dependent urban mobility subnetworks *(MD-UMNs)*

4.2.3 Reference networks

Reference networks are an important baseline against which to measure the possibility of the occurrence of certain network structures, given certain properties of empirical networks. In this study, two reference networks, which represent two extreme urban conditions that characterize urban spatial heterogeneity, were generated. Specifically, a random urban mobility network and a scale-free urban mobility network were generated, as follows:

- *Random urban mobility network (RA-UMN):* The *RA-UMN* represents the case of entirely homogeneous neighborhoods in the city, which means that all individuals' urban travel flows are purely random, without exhibiting any preferences. It is conjectured that all resources and facilities in the urban space have a relatively uniform distribution and that individuals' trips are not restricted by the urban spatial structure. This network was simulated by means of random walks between any two nodes with the same probability *p* and number of vertices N as the *G-UMN*. The degree distribution shows the characteristics of a Poisson distribution, which represents the property of homogeneity (Frieze & Karoński, 2016). In addition, the clustering coefficients are very small. This network is denoted by G_{RA-MN} in this paper.
- *Scale-free urban mobility network (SF-UMN):* The *SF-UMN* represents the case of highly heterogeneous neighborhoods in the city, which corresponds to the spatial heterogeneity derived from the relative concentrations of resources; thus, specific regions with more concentrated resources will attract a larger number of people, while other areas will experience minimal traffic. This network was generated based on preferential attachments, with the node distribution following a power law. Most nodes have only a few connections, while a few nodes possess a large number of connections. The nodes are heterogeneous, and the influence of scale disappears, which means that the network possesses the scale-free characteristic (Ferreira et al., 2018). This network is denoted by G_{SF-MN} in this paper.

4.3 Characterizing the urban mobility networks

The properties of a network are essentially characterized by a set of statistical measures (Albert & Barabási, 2002; Zeng et al., 2017), such as the node degree, node strength, and clustering coefficient. Here, we employed the essential measures of a complex network analysis to characterize the urban mobility networks. Moreover, we examined two types of scaling relations among these measures and then compared these relations between the empirical urban mobility networks and the two reference networks.

4.3.1 Statistical measures

Node degrees k_i and degree distribution $P(k)$. The node degrees k_i and the degree distribution $P(k)$ are important quantities that reveal the spatial heterogeneities of urban mobility (Jacob et al., 2017). Nodes with larger degrees represent more highly connected areas in the city. The distribution of the node degrees captures the number of nodes with a given degree *k* in the mobility network. For a given network, the node degree k_i is defined as the number of nodes to which node *i* is connected, as shown in Equation (1) (Wu & Zhang, 2011).

$$k_i = \sum_{j \in V} N(v_i, v_j) \tag{1}$$

Regarding the distribution of k, in the *SF-MN*, $P(k)$ is a fat-tailed power-law distribution, while in the *RA-MN*, $P(k)$ is a Poisson distribution. In real urban mobility networks, due to the influence of physical constraints, some deviations can be observed.

Node strengths s_i and strength distribution $P(s)$. The node strength s_i is employed to generalize the degree measure of weighted networks. The strength of node *i* is defined as the sum of the weights of the edges associated with node *i*, as shown in Equation (2).

$$s_i = \sum_{j \in V} W(v_i, v_j) \tag{2}$$

The strength distribution $P(s)$ represents the number of nodes that are associated with edges (e.g., travel flows in the urban mobility network) with the strength s; and a higher node strength suggests that this location attracts more travel flows from other locations and has the potential to be a hub node.

Local and average clustering coefficients. The local clustering coefficient of a node is a measure of the neighborhood density and captures the degree to which the neighbors of this node are linked with each other (Opsahl & Panzarasa, 2009). A high local clustering coefficient of a node indicates that individuals who visit this node will also frequently visit its neighbors. For node *i*, its local clustering coefficient $c(i)$ is the fraction of the links that are actually present among the total possible links between its neighbors. The equation for the weighted local clustering coefficient of node *i*, as defined by Barrat, et al. (2004), is

$$c_w(i) = \frac{1}{s_i(k_i-1)} \sum_{j,k} \frac{W(\ell_i,\ell_j)+W(\ell_j,\ell_k)}{2} a_{ij} a_{jk} a_{ki} \quad (3)$$

where a_{ij} are the elements of the adjacency matrix. The average clustering coefficient of all nodes, $\langle C_w \rangle$, can be applied to quantify the density of the entire network.

$$\langle C_w \rangle = \frac{\sum_{i \in V} c_w(i)}{N} \quad (4)$$

4.3.2 Scaling relations

The scaling relation examines strong trends that are observed among complex network-driven measures, such as degree, strength, and clustering coefficient. The scaling relation is a useful tool for obtaining a global trend of the mobility network of the whole city (Brú et al., 2014).

Strength s versus degree k. The node strength $s^w(k)$ averaged over all nodes of degree *k* is given by

$$s^w(k) = \frac{1}{N(k)} \sum_{i/k_i=k} s_i \quad (5)$$

The scaling relation between $s^w(k)$ and *k* is indicative of the statistical correlations between the weights of the network and the connectivities of the network (Barrat et al., 2004). This relation is given by

$$s^w(k) \sim Ak^{\beta} \quad (6)$$

In an urban mobility network, this scaling relation quantifies the visit growth of the urban nodes of different degrees. If $s^w(k)$ grows linearly with k, then $\beta = 1$. If no linear increase occurs, then $\beta \neq 1$ or $\beta = 1$ with $A \neq \langle w \rangle$. Therefore, β reflects how the travel flows per edge increase with the connectivity of the urban nodes.

Clustering coefficient c versus degree k. The weighted clustering coefficient $C_w(k)$ for nodes of a given degree k is calculated as

$$C_w(k) = \frac{1}{N(k)} \sum_{i/k_i=k} C(i) \quad (7)$$

The scaling relation between $C_w(k)$ and k indicates the correlations between the neighborhood density and the connectivity of the network (Liu et al., 2016). This relation can be generally expressed as

$$C_w(k) \propto k^{-B\alpha} \tag{8}$$

In this case of an urban mobility network, this scaling relation quantifies how spatial neighbored clusters are organized among the nodes of different degrees. A decreasing scaling relation indicates that denser neighborhoods tend to show lower connectivity.

5 Results

5.1 Properties of individuals' travel motifs

After processing the dataset, hundreds of motifs were identified from the raw mobile phone tracking data. A total of almost 91.7% of 9.7 million phone users could be characterized by 475 eligible unique motifs. A total of 2.5 million mobile phone users were omitted due to their one-stay sequences. We selected the top 9 motifs as the most frequent *motif*s for further processing. Fig. 7 depicts the chosen motif structures and their probabilities among the user population. Different colors indicate the variation in the number of nodes in a motif, which range from 2 to 5. A substantial heterogeneity exists among individuals. It can be observed that the percentage of population decreases as the number of nodes increases; the highest percentage corresponds to $n = 2$ (40.1%), followed by the motifs with $n = 3$ (25.4%) and $n = 4$ (7.5%). The most frequent motifs can be divided into two distinct motif types, i.e., the round-trip type and the multiple-trip type. The motifs of the round-trip type are *ID-2-1, ID-3-1, and ID-4-1,* while the other motifs belong to the multiple-trip type. Round-trip motifs have simpler structures and are a more effective way to satisfy the travel demands. Therefore, higher percentages of population do the round-trip motifs within their respective node number groups. The findings indicate that motifs with fewer nodes and round-trip structures are preferred by a larger number of individuals. These individuals show strong regularities of movements that tend to follow certain typical motifs. This observation is consistent with the results of Song, et al. (2010), who discovered that human movements are of the high regularity.

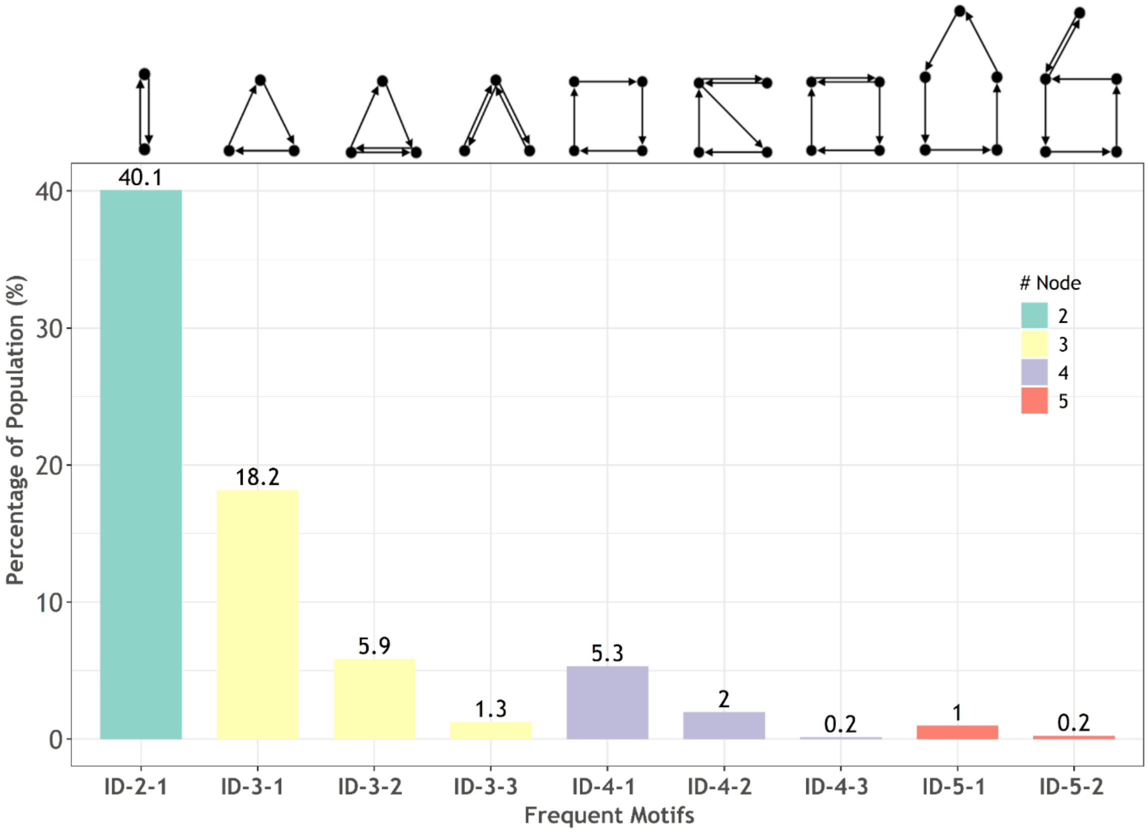

Fig. 7. Top 9 motif types extracted from the mobile phone tracking data as frequent motifs.

To uncover the spatial disparities in the top-9 motif, the entropy of the various motifs occurring at the spatial node (here, base tower) was calculated. Fig. 8 displays the distribution of the entropy values. The entropies of the motifs that occur in spatial nodes show a similar Gaussian normal distribution with a mean value of 1.15. This finding indicates that the occurrence of different type motifs is not homogeneous across the whole city. The travel motifs vary from place to place.

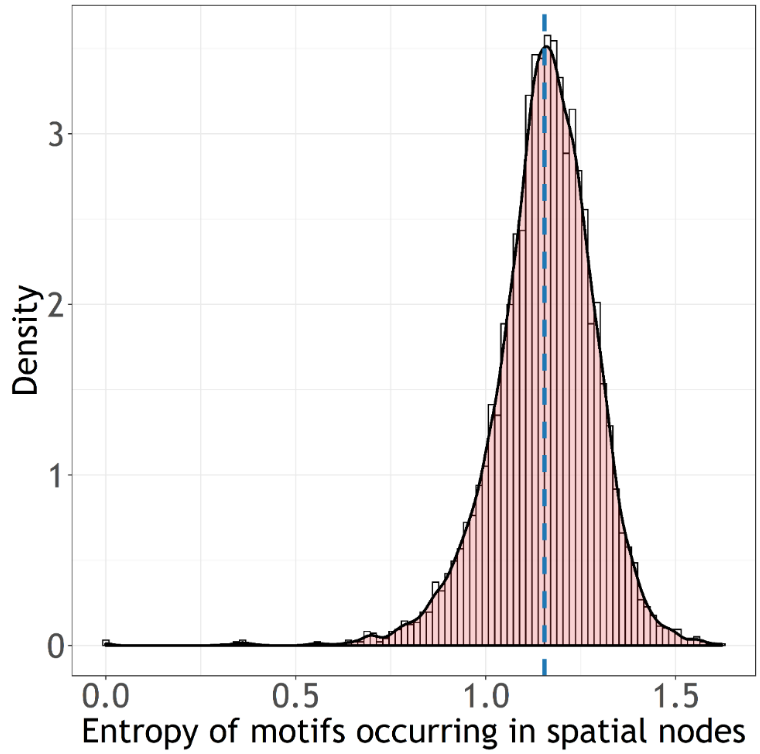

Fig. 8. Statistical distribution of the entropies of the motif probabilities.

The probabilities of occurrences of the top 9 motifs in 10 administrative districts were calculated (Fig. 9). The suburban areas hold a higher population of simpler motifs. For example, the probabilities of two-node motifs observed in the Pingshan, Dapeng, and Longgang are 0.45, 0.44, and 0.43, respectively (Table. 2). Conversely, the corresponding value for the central areas, including Luohu, Nanshan, and Futian, are 0.36, 0.36 and 0.36, respectively. However, motifs with three or more nodes occur in higher proportions in the urban areas than in the suburban areas, with values of 0.64 versus 0.40, respectively, on average. In addition, it can be observed that for each node number group, round-trip motifs hold in higher percentages in the urban centers, while multiple-trip motifs occur in higher proportions in suburbs. For instance, *ID-3-1* accounts for a proportion of 0.79 of all three-node number groups in the central areas and a proportion of 0.68 in suburban areas, while the corresponding values for *ID-3-2* are 0.17 and 0.25, respectively. We conjecture that one major reason for this finding is that people who live in the suburban areas tend to have fewer activities than those who live in the urban central areas. The result is in line with some empirical studies on the human activities in metropolitan cities, which find that residents in the suburban areas have a simple daily activity routines (Yang, Fang, Xu, et al., 2019). This finding can be further explained by the possible determination of the abundance level of urban resources (i.e., bus stations, railway stations, metros, shopping malls, hospitals parks, etc.). More abundant urban resources and higher-level socioeconomic population may have more efficient motifs.

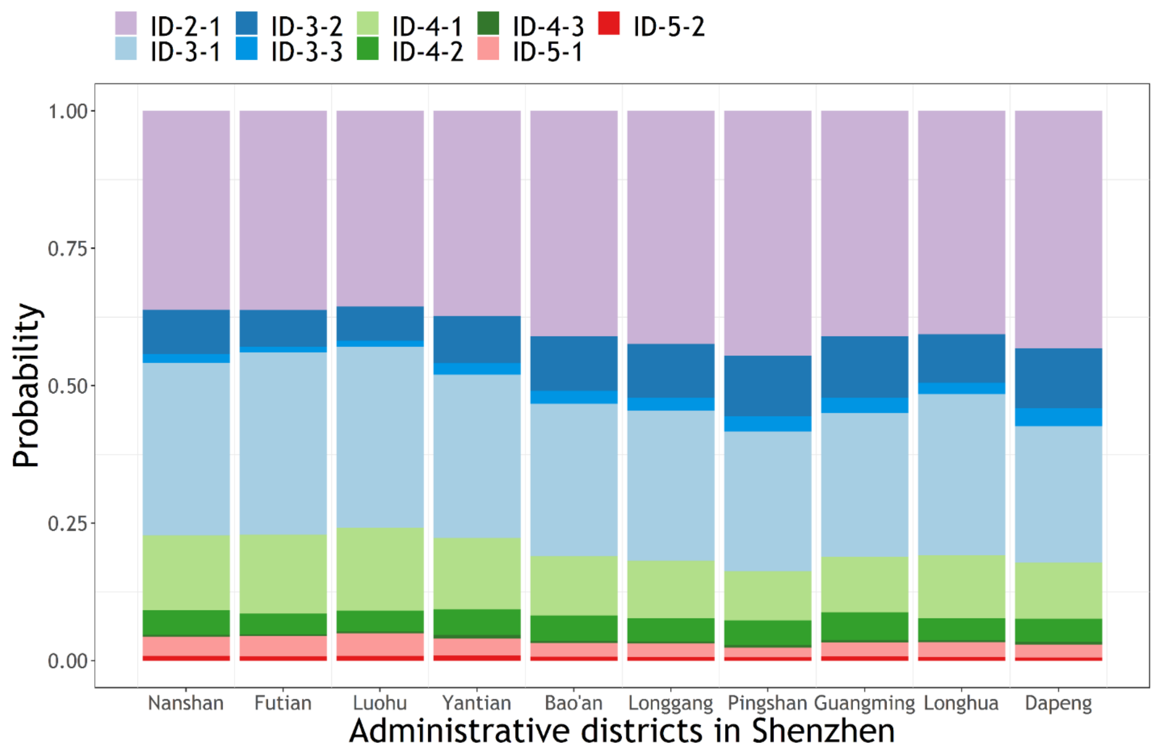

Fig. 9. Probability distributions of the 9 motif types in the 10 administrative districts of Shenzhen.

Table 2. Probabilities of the 4 motif groups in the 10 administrative districts of Shenzhen.

Administrative districts	**Two-node motifs**	**Three-node motifs**	**Four-node motifs**	**Five-node motifs**
The SEZ districts	**0.37**	**0.41**	**0.19**	**0.05**
Nanshan	0.36	0.41	0.19	0.04
Futian	0.36	0.41	0.19	0.05
Luohu	0.36	0.41	0.19	0.05

Yantian	0.38	0.41	0.19	0.04
The non-SEZ districts	**0.42**	**0.40**	**0.15**	**0.03**
Bao'an	0.41	0.40	0.16	0.03
Longgang	0.43	0.40	0.15	0.03
Pingshan	0.45	0.39	0.14	0.02
Guangming	0.41	0.40	0.16	0.03
Longhua	0.41	0.40	0.16	0.03
Dapeng	0.44	0.40	0.15	0.03

5.2 Properties of the global urban mobility network

The travel motifs of all individuals were aggregated and mapped onto the geographic space, as shown in Fig. 10. After the aggregation of all individuals' travel motifs, the *G-UMN* consists of 5,934 nodes, 2,725,000 edges, and 15,499,967 weights (i.e., total trips), which cover the entire study area.

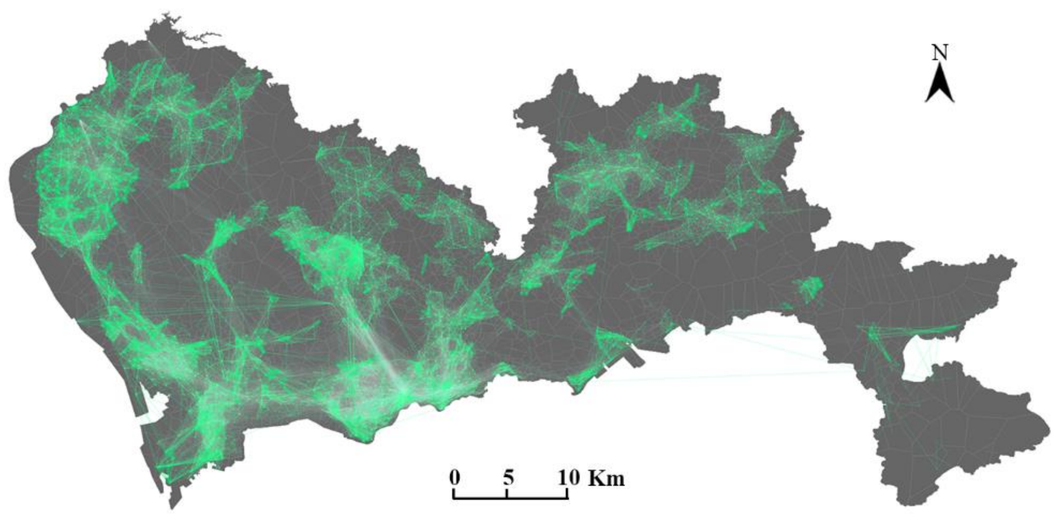

Fig. 10. Geographical mapping of the global urban mobility network (*G-UMN*).

Now, let us focus on the complex network-oriented measures that characterize the *G-UMN*. The average degree $\langle k \rangle$ of the *G-UMN* is 918.4 (including in-degree and out-degree), which indicates that, on average, each base tower is connected with 460 other base towers by individuals' movements and that the connectivity of the mobility network is relatively high. Fig. 11(a) shows the degree distribution $P(k)$ on a log-linear plot. The red points correspond to the empirical data that are aggregated to form the *G-UMN*, and the purple line corresponds to an exponential fit, which is shown by a straight line. We also show the Poisson distribution that is predicted with the same average degree $\langle k \rangle$ as the *G-UMN* (green line) and a similarly predicted power-law distribution (yellow line). It can be observed that the empirical $P(k)$ obeys an exponential distribution ($P(k) \propto e^{-0.001k}$). Fig. 11(b) shows the strength distribution $P(s)$ on a log-linear plot. Similarly, $P(s)$ is also fitted with an exponential distribution ($P(s) \propto e^{-0.002s}$). The exponential distribution also has an obvious long tail, which indicates a heterogeneous spatial pattern. The deviation of the empirical behavior from Poisson distribution and power-law distribution suggests that the *G-UMN* can be characterized neither by a completely random spatial distribution nor by a purely scale-free spatial distribution. In addition, the *G-UMN* shows a large average clustering coefficient ($\langle C_w \rangle = 0.59$), which is significantly larger than that of the *RA-UMN* ($\langle C_w^{RA-MN} \rangle = 0.15$); the *G-UMN* is rather clustered and is far from a random distribution. These findings imply that the urban mobility in the study area is heterogeneous: some areas attract a large number of travel flows, while other areas are visited by few individuals. Residents tend to travel more frequently to nearby locations, and cross-regional travels are rare. Thus, the *G-UMN* forms locally clustered areas.

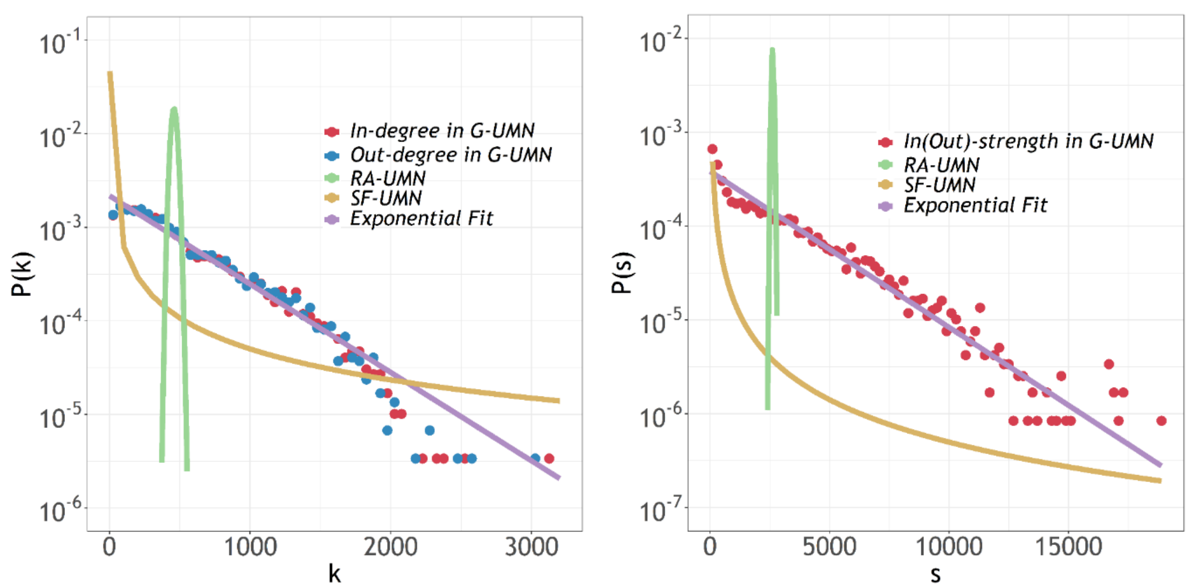

Fig. 11. Properties of the *G-UMN*. (a) Distribution of the node degrees. (b) Distribution of the node strengths.

To further investigate how the *G-UMN* has developed on a global scale, we analyzed the scaling relation between the number of trips (strength) and the number of nodes (degree). In Fig. 12(a), the red points and blue points represent the in-degree strength and out-degree strength, respectively, of each node in the *G-UMN*. The profile of strength versus degree resembles a straight line when plotted in logarithmic coordinates, as shown by the purple line, which corresponds to $s^w(k) \sim Ak^{\beta}$ with $\beta = 1.24$, whereas the green line corresponds to the properties of the *RA-UMN* with $\beta = 1$. The observation of $\beta > 1$ suggests that trips that originate or end in highly connected areas occupy more flows than they would occupy in a random network. More importantly, the volume of travel trips will have an increase at a faster rate than the increase of connectivity of urban areas. In other words, more highly connected areas in the city can attract a disproportionately larger number of travel flows. The finding suggests that the improvement of the connectivity in urban areas will accelerate population flows.

The other scaling relation of interest is that between the clustering coefficient of a spatial node and its degree. Fig. 12(b) shows the empirical behavior of the *G-UMN* in terms of clustering coefficients versus degrees. The blue points and red points correspond to $C_w(k)$ and $C(k)$, respectively, and the purple line and cyan dotted line represent the corresponding power-law fits, where $C_w(k) \propto k^{-0.15}$ and $C(k) \propto k^{-0.22}$, respectively. Fig. 12(b) indicates that $C(k) < C_w(k)$, which means that nodes of higher degrees accumulate a larger number of travel flows. For comparison, we also presented green points and a yellow dotted line to show the relation that characterizes the *SF-UMN* ($C_w(k) \propto const$). The empirical observation of a decreasing relation indicates that urban areas with denser neighborhoods do not tend to show higher connectivity; instead, the opposite tendency is observed.

As proven by the work of Dorogovtsev, et al. (2002), networks that exhibit scaling relations of the form $C_w(k) \propto k^{-B\alpha}$ are considered hierarchical networks, where a scaling exponent of $\alpha = 1$ indicates a complete hierarchy. A hierarchical structure implies that sparsely connected areas tend to be part of highly clustered areas, where the links between the different highly clustered neighborhoods are maintained by only a few hubs (Ravasz & Barabási, 2003). A few local hubs attract quantities of travel flows and form hierarchically polycentric groups within the city. Each group is internally heterogeneous.

Here, the *G-UMN* is empirically observed to obey this relation with $\alpha = 0.15$. This finding suggests that the city possesses an evolving hierarchically polycentric structure, which coincides with the reality of the fast-growing city in the world (Liu et al., 2016).

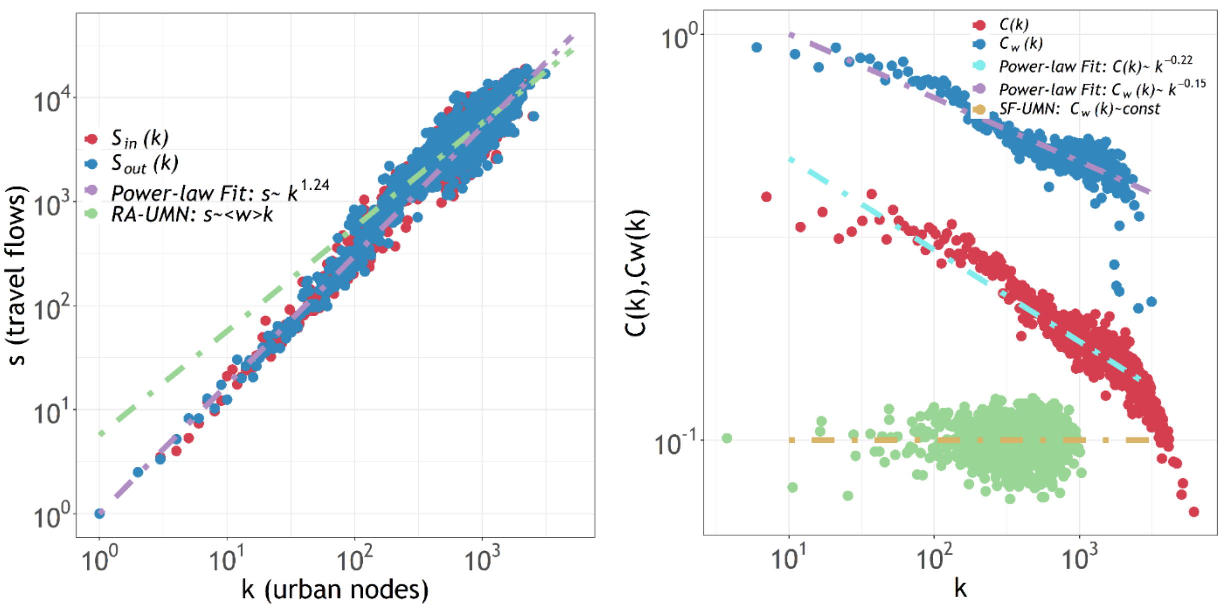

Fig. 12. (a) Scaling relation between strength and degree. (b) Scaling relation between clustering coefficient and degree.

5.3 Differences in the properties of the motif-dependent urban mobility networks (*MD-UMNs*)

Based on the nine extracted frequent motifs, we constructed nine *MD-UMNs*. We further presented a comparative quantitative analysis of the statistical measures and scaling relations of the *MD-UMNs*, which reflects the impacts of the heterogeneities of individual travel motifs and the differences in the urban spatial structure. Table 3 summarizes the results for the statistical properties of these nine networks. The total number of nodes for all 9 *MD-UMNs* was set to 5,926. There are differences among these network statistical properties. The top four *MD-UMNs* are the *ID-2-1,* the *ID-3-1,* the *ID-3-2* and the *ID-4-1* networks. The *ID-5-1* and *ID-5-2* networks are relatively small. Specifically, for the top 2 *MD-UMNs,* i.e., *ID-2-1* and *ID-3-1,* which were constructed based on the two-node round-trip motif and the three-node round-trip motif, respectively, the average degree $\langle k \rangle$ of the *ID-2-1* network($\langle k \rangle = 450.36$) is slightly smaller than that of the *ID-3-1* network ($\langle k \rangle = 464.78$), while the average strength of the *ID-2-1* network ($\langle s \rangle = 2064.97$) is nearly two times greater than that of the *ID-3-1* network ($\langle s \rangle = 1406.55$). These observations indicate that these people had specific spatial dispersion patterns in terms of motifs. The *ID-2-1* network has a more spatially aggregated distribution of interacted strengths, while *ID-3-1* network has a more dispersed distribution of interacted strengths. This is related to the finding abovementioned in section 5.1 that people in different areas have different activity demands according to the urban abundance and socioeconomic levels.

Fig. 13 illustrates the distributions of the node strengths of the *MD-UMNs* on a log-linear plot. The strength values were normalized with respect to the average weights $\langle w \rangle$. The points in different colors correspond to different *MD-UMNs*. The distributions of all 9 *MD-UMNs* show similar patterns, which are well fitted by exponential distributions; however, there are differences in the rate parameters of the fitted distributions. The fitted rate parameters range from 0.006 to 1, as summarized in Table 3. The 4 round-trip *MD-UMN*s, i.e., *ID-2-1*, *ID-3-1*, *ID-4-1*, and *ID-5-1* occupy the highest proportion in its respective node number group. *ID-2-1* and *ID-3-1* have the lowest decay rate (0.006), *ID-4-1* has the median decay rate (0.01), and *ID*-5-1 network has the highest decay rate (0.06). The variations in parameters suggest that the spatial heterogeneities of urban mobility exist and differentiate when considering different travel motif types. *ID-5-1* corresponds to more concentrated spatial patterns of hub nodes and fewer hub nodes than *ID-2-1*. The larger is the node number, the more complex is the individual motif, and thus, the more centralized are the spatial patterns of the urban mobility networks. The results further imply the hypothesis of complex influences of the structures of individual travel on the spatial patterns of urban mobility.

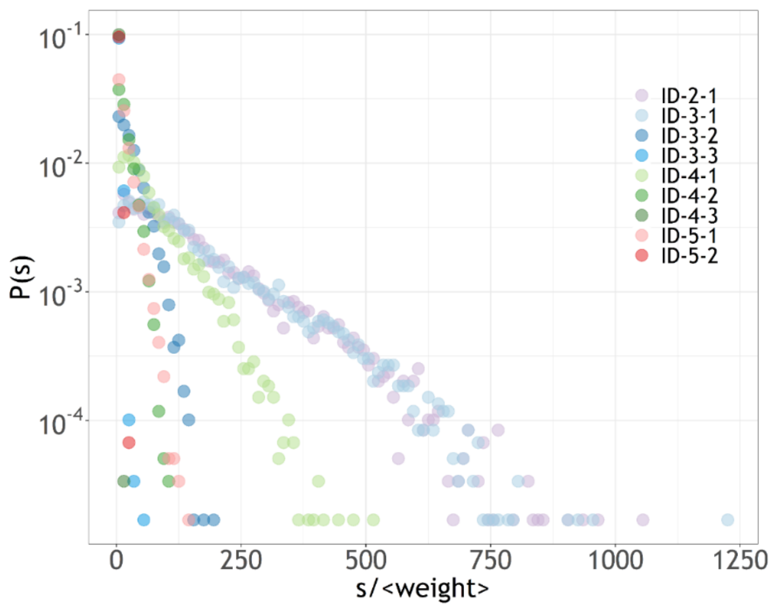

Fig. 13. Distributions of the node strengths for the nine *MD-UMNs*.

Table 3. Statistical properties of the *G-UMN* and the 9 *MD-UMNs*

	G-UMN	***ID-2-1***	***ID-3-1***	***ID-3-2***	***ID-3-3***	***ID-4-1***	***ID-4-2***	***ID-4-3***	***ID-5-1***	***ID-5-2***
	-	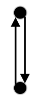	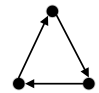	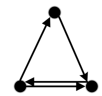	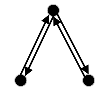	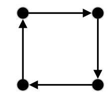	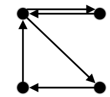	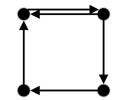	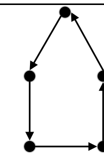	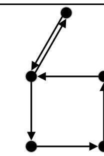
Number of individuals	5655782	3059250	1389202	447220	97395	406024	150299	11485	75937	18970
Number of travel flows	15499967	6118500	4167606	1788880	486975	1624096	751495	68910	379685	113820
Number of edges	2725000	1334410	1377148	431392	111132	741173	291023	38166	247063	78261
Ave. node degree	919.8	450.36	464.78	145.59	37.51	250.14	98.22	12.88	83.38	26.41
Ave. node in-degree	459.8	225.18	232.39	72.80	18.75	125.07	49.11	6.44	41.69	13.21
Ave. strength	5231.17	2064.97	1406.55	603.74	164.35	548.13	253.63	23.26	128.14	38.41
Ave. in-strength	2615.59	1032.48	703.27	301.87	82.18	274.06	126.81	11.63	64.07	19.21
Ave. weight	5.69	4.59	3.03	4.15	4.38	2.19	2.58	1.81	1.54	1.45
Ave. undirected cc	0.21	0.23	0.28	0.17	0.21	0.22	0.17	0.17	0.14	0.13
Ave. weighted cc	0.60	0.41	0.54	0.38	0.58	0.45	0.43	0.30	0.33	0.29
Rate parameter in strength distribution	0.002	0.006	0.006	0.03	0.25	0.01	0.06	1	0.06	0.32

To confirm the abovementioned hypothesis, we further analyzed the spatial patterns of the node strengths of the *MD-UMNs* by mapping the strength values of the nodes onto a geographic space. Because the strength values vary over several orders of magnitude, we normalized them using the min-max normalization method. Each strength value is normalized by subtracting the minimum strength and dividing by the difference between the maximum strength and the minimum strength to rescale the range of the strength values to [0, 1]. The spatial distributions of the normalized strengths of the top 4 *MD-UMN*s are illustrated in Fig. 14. The red color indicates that the nodes have higher strengths, and thus, act as hub nodes, whereas the yellow color represents smaller values. Moreover, the larger the circle size is, the higher the strength is. The results reflect the differences in the spatial configuration of the hub nodes. In terms of *ID-2-1*, Fig. 14(a) reveals that hub nodes are relatively well distributed in the urban central districts. Regarding *ID-3-1*, Fig. 14(b) demonstrates that a cluster of hub nodes is located in the suburban districts. The central areas have a low level of strength nodes, which is quite different from those indicated by the *ID-2-1* network. Regarding the *ID-4-1* network, the pattern is similar to that derived from the *ID-3-1* network (Fig. 14(c)). For the *ID-5-1* network, the hub nodes are concentrated in the central districts (Fig. 14(d)). These observations support the hypothesis that the different spatial patterns of urban mobility are caused by the structures of individual travels. The spatial pattern of the hub nodes in *ID-2-1* is relatively scattered, whereas that in *ID-5-1* is relatively centralized. This finding is consistent the findings of related studies, which indicates a strong positive correlation between the number of visited locations and the scope of the spatial dispersion distribution (Xu et al., 2015).

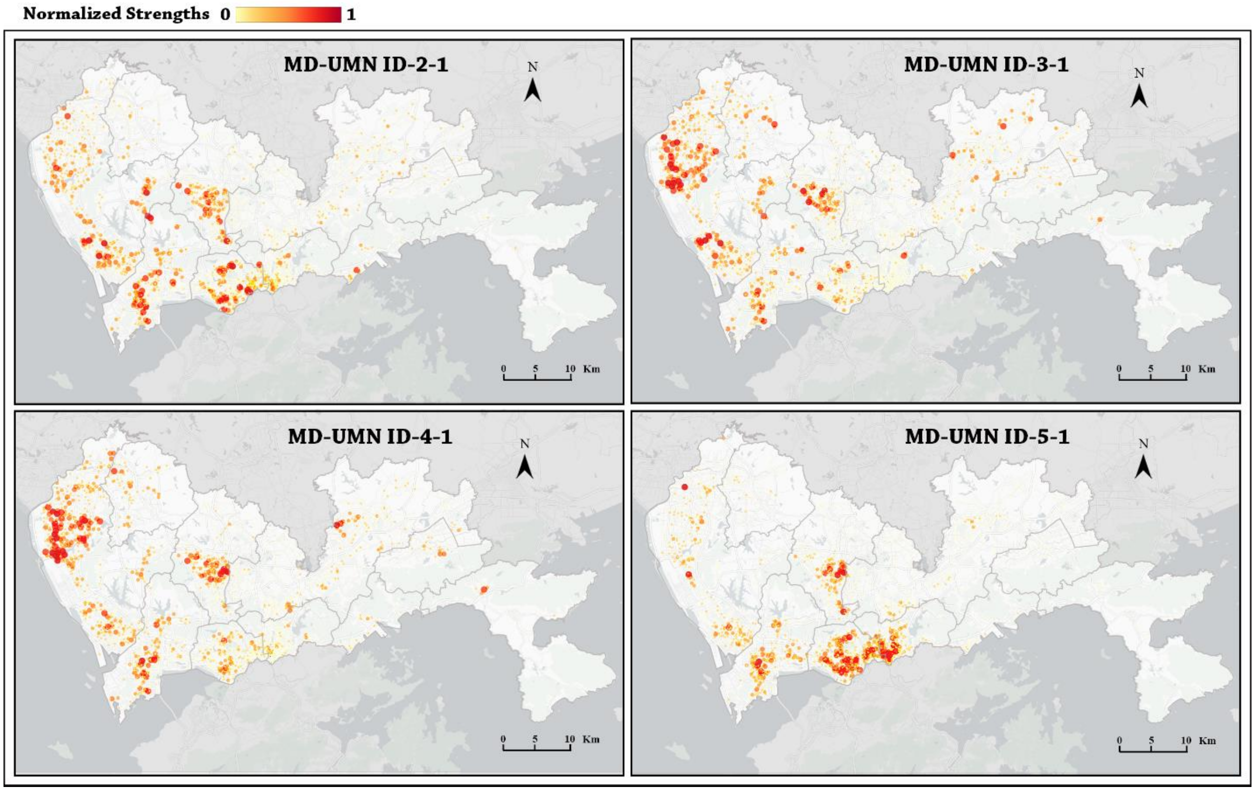

Fig. 14. Spatial distributions of the normalized node strengths in the *MD-UMNs* that correspond to motifs *ID-2-1*, *ID-3-1*, *ID-4-1*, and *ID-5-1.*

The results of the scaling relations between degree and strength in the *MD-UMNs* are displayed in Fig. 15(a). For this analysis, the strength values were normalized with respect to the average weight $\langle w \rangle$. Points of different colors represent empirical data from different *MD-UMNs*, and the black dotted line corresponds to the linear scaling relation in the *RA-UMN* with $\beta = 1$. The scaling exponents β, which are listed in Table 4, range from 1.08 to 1.33. All of these β are larger than 1. However, there are deviations from the scaling relation. For smaller degree values, the strength increases super-linearly with the node degree, which indicates that the strengths of the urban nodes increase at a faster rate than their degrees when the node degrees are low. This increasing trend, however, shows a linear increase for larger degree values, which suggests that an urban area of higher degree tends to proportionately attract more travel flows (of which it may be either the origin or the destination).

The results of the scaling relations of the local weighted clustering coefficients with respect to the node degrees in the *MD-UMN*s are shown in Fig. 15(b). Points in different colors correspond to different *MD-UMNs*. As in the case of the *G-UMN*, this scaling relation can always be fitted with a power law for any *MD-UMN*. The structures of the *MD-UMNs* differ only in the value of the scaling exponent α, and do not differ in the general form of the scaling relation. The scaling exponents α, which are listed in Table 4, range from 0.13 to 0.42. All of these α are larger than 0. These results demonstrate that all of these networks have a decreasing scaling relation between the clustering coefficients and the node degrees. Different values of α imply different evolutionary states of structures of urban mobility networks. Smaller values of α indicate more random properties of networks, while larger values mean more hierarchical properties. The results suggest that the *MD-UMN*s *ID-2-1* and *ID-3-1* (for which $\alpha = 0.13$ and 0.21, respectively) tend to show more randomness, while the *ID-4-3* and *ID-3-3* (for which $\alpha = 0.40$ and 0.42, respectively) tend to be more hierarchical; the other *MD-UMNs* lie somewhere in between these results.

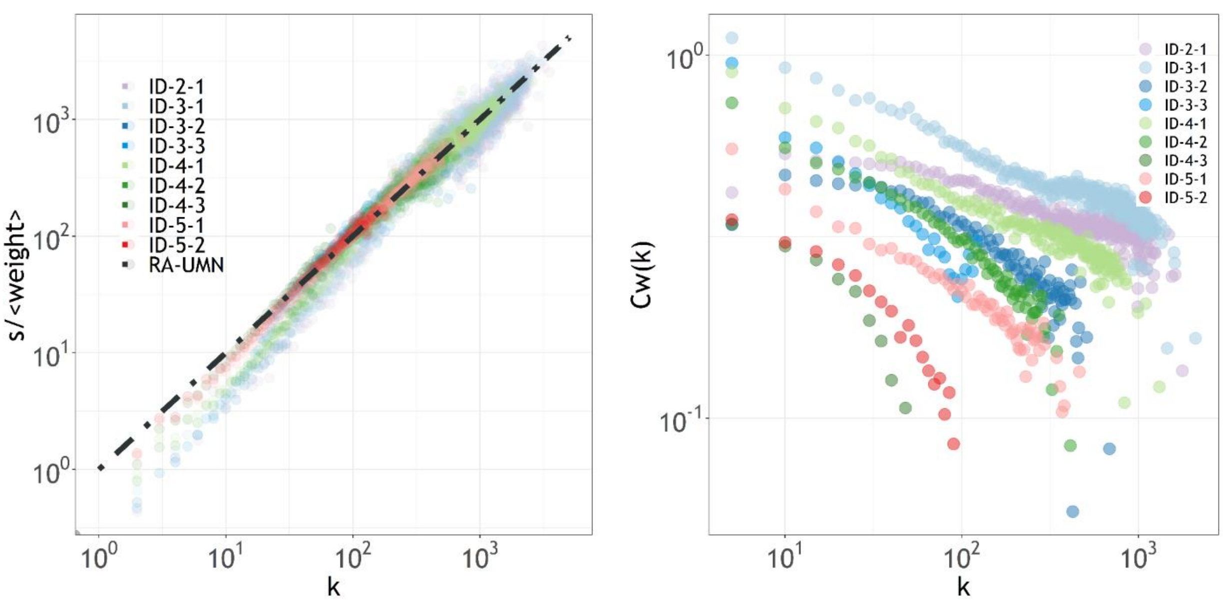

Fig. 15. (a) Scaling relations between degree and strength for different *MD-UMNs*. (b) Scaling relations of the local clustering coefficients $C_w(k)$ as functions of the degree *k*.

Table 4. Fitting results for the scaling relations of the *G-UMN* and 9 *MD-UMNs*

	G-UMN	***ID-2-1***	***ID-3-1***	***ID-3-2***	***ID-3-3***	***ID-4-1***	***ID-4-2***	***ID-4-3***	***ID-5-1***	***ID-5-2***
		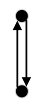	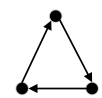	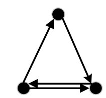	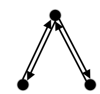	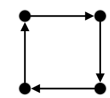	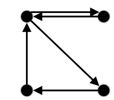	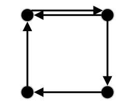	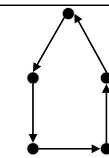	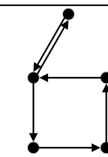
$\boldsymbol{\beta}$	1.23	1.22	1.16	1.23	1.33	1.12	1.16	1.18	1.08	1.10
$\boldsymbol{\alpha}$ ***(weighted)***	0.16	0.13	0.21	0.22	0.42	0.24	0.33	0.40	0.31	0.38
$\boldsymbol{\alpha}$ ***(undirected)***	0.22	0.20	0.27	0.32	0.67	0.29	0.44	0.57	0.36	0.50

6 Discussion and conclusion

Quantitative measures for characterizing urban mobility networks have the potential to greatly advance a deeper understanding of urban mobility. By rethinking the recent science of “complex networks” and motivated by the increasing availability of big human tracking data, this paper has developed an overarching framework for characterizing urban mobility networks from the perspective of complex networks. In contrast to existing measures that focus on the aggregation of human mobility, this paper explores the impacts of the heterogeneity of individual travels and constructs multiple urban mobility networks to represent the corresponding heterogeneous characteristics. These urban mobility networks were investigated by computing statistical measures and modelling scaling relations that are based on complex network theory, which allows us to assess how the mobility networks have developed. Considering Shenzhen, China as an example, we have experimentally demonstrated the effectiveness of the proposed framework.

By investigating the properties of individuals’ travel motifs, the analysis results demonstrated that the individual travel motifs are structurally and spatially heterogeneous. This result conforms to the findings that population segregation, facility density and transport accessibility in different areas of the city are suggested as potential factors in the variation of motif distributions (Allen et al., 2012; Chen et al., 2018; Gao et al., 2018). Due to the abundance of the urban resources and accessible transport infrastructures in the central areas, residents tend to visit a larger number of places and exhibit more efficient travel motifs in these regions. Most low-socioeconomic-level population live in the suburbs of the city in China, which is different from the findings of many Western studies that these population concentrate in the urban centers (Mieszkowski & Mills, 1993). These population groups usually have less activity demands. This finding reinforces the finding that the spatial allocation of urban resources is an important factor that influence the motif choices of different population groups.

The statistical measures and scaling relations of the *G-UMN* enable us to better understand to what status an urban mobility network develops. The results stated that travel that originates or ends in highly connected urban areas occupies a larger number of flows, and forms some locally clustered areas. Consequently, less highly connected areas in suburban and outskirt areas attract fewer travel flows; however, areas with denser neighborhoods show lower connectivity. The finding indicated that residents who live in the suburban areas tend to have fewer activity choices than those who live in the urban central areas. In addition, the results also implied that the *G-UMN of* a fast-developing city is undergoing an evolving hierarchically polycentric structure, in which it is developing from a random network into a scale-free network. Locally clustered areas may cause spatial heterogeneity in urban mobility and insufficient mobility issue, especially in the outskirts and peripheral areas. Therefore, the role of facility accessibility in these areas is central to improve the urban and transportation planning. On the one hand, it is necessary to build additional public transport and public service facilities to encourage diversified travels in suburban or outskirt areas. On the other hand, to avoid the partial congestion caused by the extreme attraction of urban hubs, when planning the establishment of urban infrastructures, policy makers should fully consider how to retain the hierarchical and polycentric structure of urban mobility. For instance, connecting central hubs with more expressways and ensuring that alleys are unblocked within each district are effective ways to maintain the polycentric structure.

Finally, the exploration of the differences in the properties among the *MD-UMNs* provided insights to the differences in the multifaced urban mobility networks and indicated that the spatial heterogeneities among different motif types. The results suggested that the urban network structures are influenced by individual mobility. The behavioral differences in network properties and spatial heterogeneities of urban mobility vary across the *MD-UMNs*. Generally, simple motifs exhibit relatively dispersed spatial patterns, while more complex motifs are associated with highly clustered and centralized structures. These findings emphasized the spatial patterns of urban mobility networks for future policymaking. The implication lies in the elucidation of the structural complexity of urban mobility networks as characterized by the diversity of individual mobility. The complex motifs easily form highly clustered network structures, such as *ID-5-1* in urban central areas. In many metropolitan cities, the trend of spatial inequality in urban resources due to the urban agglomeration effect(Fang & Yu, 2017; Partridge & Rickman, 2008), which exacerbates the scarcity of urban resources in the suburbs. This will continue to impact the urban form and structure. Therefore, allocating resources in a more dispersed manner to satisfy the complex travel demands of the citizens can effectively reduce the overload of hub nodes that are centralized in special regions.

The results not only provide a promising bridge from complex network properties to urban mobility patterns but also imply potential urban planning policies. Our primary findings are complementary to urban studies but possess a different but typical urban context in light of urban development path. Some recent studies indicated there are polycentric metropolitan form with tiers of hierarchical centers in cities of Western countries, such as the San Francisco (Cervero & Wu, 1997) and London(Roth et al., 2011). China, especially other first-tier cities, including Beijing(Deng et al., 2019), and Shanghai(Xi Liu et al., 2015), has manifested a similar pattern. Despite its similarity, China has its unique policy guidance and urban-rural gap, resulting in different urbanization processes. For example, Shenzhen is a fast-developing city and its distribution of urban resources is more affected by the policy restrictions in early years and the differences between centers and suburbs is larger than that in Western cities. Thus, these differences reinforce that the future urban-oriented policies should be more targeted among cities considering the policy restrictions and development stages. For instance, whether maintaining the hierarchical structures or reducing urban hubs in a fast-developing city or a well-developed city should be discussed city by city. Our study needs to be extended of course to other urban areas, which will complement and enrich the urban studies.

Further work is needed to fully explore the potential applications of the proposed approach. First, we understand that the lack of a longer-term dataset influences the robustness of the results and limits their validity. However, the increasing availability of suitable data sources may solve this problem. Furthermore, with the availability of time-series data, our proposed framework may be extended to achieve the dynamic monitoring of the evolution of urban systems. Last, our proposed measures are rather simple and may be enhanced to include more comprehensive measures, such as statistics that consider the social perspective and capture dynamical and topological features. Beyond these possibilities, spatial influences, such as travel distance, could also be considered.

Declaration of Competing Interests

The authors declare no conflicts of interest.

References

Agryzkov, T., Martí, P., Tortosa, L., & Vicent, J. F. (2017). Measuring urban activities using Foursquare data and network analysis: A case study of Murcia (Spain). *International Journal of Geographical Information Science*, *31*(1), 100–121. https://doi.org/10.1080/13658816.2016.1188931

Albert, R., & Barabási, A.-L. (2002). Statistical mechanics of complex networks. *Reviews of Modern Physics*, *74*(1), 47–97. https://doi.org/10.1103/RevModPhys.74.47

Alexander, L., Jiang, S., Murga, M., & González, M. C. (2015). Origin–destination trips by purpose and time of day inferred from mobile phone data. *Transportation Research Part C: Emerging Technologies*, *58, Part B*, 240–250. 75. https://doi.org/10.1016/j.trc.2015.02.018

Allen, J., Browne, M., & Cherrett, T. (2012). Investigating relationships between road freight transport, facility location, logistics management and urban form. *Journal of Transport Geography*, *24*, 45–57. https://doi.org/10.1016/j.jtrangeo.2012.06.010

Bachir, D., Khodabandelou, G., Gauthier, V., El Yacoubi, M., & Puchinger, J. (2019). Inferring dynamic origin-destination flows by transport mode using mobile phone data. *Transportation Research Part C: Emerging Technologies*, *101*, 254–275. https://doi.org/10.1016/j.trc.2019.02.013

Barabási, A.-L. (2005). The origin of bursts and heavy tails in human dynamics. *Nature*, *435*(7039), 207. https://doi.org/10.1038/nature03459

Barabási, A.-L., & Albert, R. (1999). Emergence of Scaling in Random Networks. *Science*, *286*(5439), 509–512. https://doi.org/10.1126/science.286.5439.509

Barrat, A., Barthélemy, M., Pastor-Satorras, R., & Vespignani, A. (2004). The architecture of complex weighted networks. *Proceedings of the National Academy of Sciences*, *101*(11), 3747–3752. https://doi.org/10.1073/pnas.0400087101

Barthélemy, M. (2011). Spatial networks. *Physics Reports*, *499*(1–3), 1–101. https://doi.org/10.1016/j.physrep.2010.11.002

Batty, M. (2008). The Size, Scale, and Shape of Cities. *Science*, *319*(5864), 769–771. https://doi.org/10.1126/science.1151419

Belyi, A., Bojic, I., Sobolevsky, S., Sitko, I., Hawelka, B., Rudikova, L., Kurbatski, A., & Ratti, C. (2017). Global multi-layer network of human mobility. *International Journal of Geographical Information Science*, *31*(7), 1381–1402. https://doi.org/10.1080/13658816.2017.1301455

Bettencourt, L. M. A. (2013). The Origins of Scaling in Cities. *Science*, *340*(6139), 1438–1441. https://doi.org/10.1126/science.1235823

Blondel, V. D., Decuyper, A., & Krings, G. (2015). A survey of results on mobile phone datasets analysis. *EPJ Data Science*, *4*(1), 10. 69. https://doi.org/10.1140/epjds/s13688-015-0046-0

Bokányi, E., Kallus, Z., & Gódor, I. (2019). Collective sensing of evolving urban structures: From activity-based to content-aware social monitoring. *Environment and Planning B: Urban Analytics and City Science*, 239980831984876. https://doi.org/10.1177/2399808319848760

Brockmann, D., Hufnagel, L., & Geisel, T. (2006). The scaling laws of human travel. *Nature*, *439*(7075), 462–465. https://doi.org/10.1038/nature04292

Brú, A., Alós, E., Nuño, J. C., & de Dios, M. F. (2014). Scaling in complex systems: A link between the dynamics of networks and growing interfaces. *Scientific Reports*, *4*(1), 7550. https://doi.org/10.1038/srep07550

Calabrese, F., Di Lorenzo, G., Liu, L., & Ratti, C. (2011). Estimating Origin-Destination Flows Using Mobile Phone Location Data. *IEEE Pervasive Computing*, *10*(4), 36–44. https://doi.org/10.1109/MPRV.2011.41

Calabrese, F., Ferrari, L., & Blondel, V. D. (2014). Urban Sensing Using Mobile Phone Network Data: A Survey of Research. *ACM Computing Surveys*, *47*(2), 1–20. https://doi.org/10.1145/2655691

Cao, J., Li, Q., Tu, W., & Wang, F. (2019). Characterizing preferred motif choices and distance impacts. *PLOS ONE*, *14*(4), e0215242. https://doi.org/10.1371/journal.pone.0215242

Cervero, R., & Wu, K.-L. (1997). Polycentrism, Commuting, and Residential Location in the San Francisco Bay Area. *Environment and Planning A: Economy and Space*, *29*(5), 865–886. https://doi.org/10.1068/a290865

Chen, B. Y., Wang, Y., Wang, D., Li, Q., Lam, W. H. K., & Shaw, S.-L. (2018). Understanding the Impacts of Human Mobility on Accessibility Using Massive Mobile Phone Tracking Data. *Annals of the American Association of Geographers*, *108*(4), 1115–1133. https://doi.org/10.1080/24694452.2017.1411244

Cheng, J., Bertolini, L., Clercq, F. le, & Kapoen, L. (2013). Understanding urban networks: Comparing a node-, a density- and an accessibility-based view. *Cities*, *31*, 165–176. https://doi.org/10.1016/j.cities.2012.04.005

Chi G., Thill J.-C., Tong D., Shi L., & Liu Y. (2016). Uncovering regional characteristics from mobile phone data: A network science approach. *Papers in Regional Science*, *95*(3), 613–631. https://doi.org/10.1111/pirs.12149

De Montis, A., Barthelemy, M., Chessa, A., & Vespignani, A. (2005). The structure of Inter-Urban traffic: A weighted network analysis. *ArXiv:Physics/0507106*. http://arxiv.org/abs/physics/0507106

Deng, Y., Liu, J., Liu, Y., & Luo, A. (2019). Detecting Urban Polycentric Structure from POI Data. *ISPRS International Journal of Geo-Information*, *8*(6), 283. https://doi.org/10.3390/ijgi8060283

Dorogovtsev, S. N., Goltsev, A. V., & Mendes, J. F. F. (2002). Pseudofractal scale-free web. *Physical Review E*, *65*(6), 066122. https://doi.org/10.1103/PhysRevE.65.066122

Fang, C., & Yu, D. (2017). Urban agglomeration: An evolving concept of an emerging phenomenon. *Landscape and Urban Planning*, *162*, 126–136. https://doi.org/10.1016/j.landurbplan.2017.02.014

Ferreira, D. L., Nunes, B. A. A., & Obraczka, K. (2018). Scale-Free Properties of Human Mobility and Applications to Intelligent Transportation Systems. *IEEE Transactions on Intelligent Transportation Systems*, *19*(11), 3736–3748. https://doi.org/10.1109/TITS.2018.2866970

Frieze, A., & Karoński, M. (2016). *Introduction to Random Graphs* (1 edition). Cambridge University Press.

Gao, Q.-L., Li, Q.-Q., Yue, Y., Zhuang, Y., Chen, Z.-P., & Kong, H. (2018). Exploring changes in the spatial distribution of the low-to-moderate income group using transit smart card data. *Computers, Environment and Urban Systems*, *72*, 68–77. https://doi.org/10.1016/j.compenvurbsys.2018.02.006

Gao, S., Liu, Y., Wang, Y., & Ma, X. (2013). Discovering Spatial Interaction Communities from Mobile Phone Data. *Transactions in GIS*, *17*(3), 463–481. 13. https://doi.org/10.1111/tgis.12042

Gómez, S., Fernández, A., Meloni, S., & Arenas, A. (2018). Impact of origin-destination information in epidemic spreading. *ArXiv:1804.02581 [Cond-Mat, Physics:Physics]*. http://arxiv.org/abs/1804.02581

González, M. C., Hidalgo, C. A., & Barabási, A.-L. (2008). Understanding individual human mobility patterns. *Nature*, *453*(7196), 779–782. 5. https://doi.org/10.1038/nature06958

Guidotti, R., Monreale, A., Rinzivillo, S., Pedreschi, D., & Giannotti, F. (2016). Unveiling mobility complexity through complex network analysis. *Social Network Analysis and Mining*, *6*(1), 59. https://doi.org/10.1007/s13278-016-0369-2

Hamedmoghadam, H., Ramezani, M., & Saberi, M. (2019). Revealing latent characteristics of mobility networks with coarse-graining. *Scientific Reports*, *9*(1), 7545. https://doi.org/10.1038/s41598-019-44005-9

Hasan, S., Schneider, C. M., Ukkusuri, S. V., & González, M. C. (2012). Spatiotemporal Patterns of Urban Human Mobility. *Journal of Statistical Physics*, *151*(1–2), 304–318. 70. https://doi.org/10.1007/s10955-012-0645-0

Hossmann, T., Spyropoulos, T., & Legendre, F. (2011). *A complex network analysis of human mobility*. 876–881. https://doi.org/10.1109/INFCOMW.2011.5928936

Huang, Z., Wang, P., Zhang, F., Gao, J., & Schich, M. (2018). A mobility network approach to identify and anticipate large crowd gatherings. *Transportation Research Part B: Methodological*, *114*, 147–170. https://doi.org/10.1016/j.trb.2018.05.016

Jacob, R., Harikrishnan, K. P., Misra, R., & Ambika, G. (2017). Measure for degree heterogeneity in complex networks and its application to recurrence network analysis. *Royal Society Open Science*, *4*(1), 160757. https://doi.org/10.1098/rsos.160757

Jiang, B., Yin, J., & Zhao, S. (2009). Characterizing the human mobility pattern in a large street network. *Physical Review E*, *80*(2), 021136. https://doi.org/10.1103/PhysRevE.80.021136

Krings, G., Calabrese, F., Ratti, C., & Blondel, V. D. (2009). Urban gravity: A model for inter-city telecommunication flows. *Journal of Statistical Mechanics: Theory and Experiment*, *2009*(07), L07003. https://doi.org/10.1088/1742-5468/2009/07/L07003

Lera, I., Pérez, T., Guerrero, C., Eguíluz, V. M., & Juiz, C. (2017). Analysing human mobility patterns of hiking activities through complex network theory. *PLOS ONE*, *12*(5), e0177712. https://doi.org/10.1371/journal.pone.0177712

Lim, C., Kim, K.-J., & Maglio, P. P. (2018). Smart cities with big data: Reference models, challenges, and considerations. *Cities*, *82*, 86–99. https://doi.org/10.1016/j.cities.2018.04.011

Liu, Xi, Gong, L., Gong, Y., & Liu, Y. (2015). Revealing travel patterns and city structure with taxi trip data. *Journal of Transport Geography*, *43*, 78–90. https://doi.org/10.1016/j.jtrangeo.2015.01.016

Liu, Xingjian, Derudder, B., & Wu, K. (2016). Measuring Polycentric Urban Development in China: An Intercity Transportation Network Perspective. *Regional Studies*, *50*(8), 1302–1315. https://doi.org/10.1080/00343404.2015.1004535

Liu, Y., Zhao, C., Wang, X., Huang, Q., Zhang, X., & Yi, D. (2016). The degree-related clustering coefficient and its application to link prediction. *Physica A: Statistical Mechanics and Its Applications*, *454*, 24–33. https://doi.org/10.1016/j.physa.2016.02.014

Liu, Y., Kang, C., Gao, S., Xiao, Y., & Tian, Y. (2012). Understanding intra-urban trip patterns from taxi trajectory data. *Journal of Geographical Systems*, *14*(4), 463–483. https://doi.org/10.1007/s10109-012-0166-z

Liu, Y., Sui, Z., Kang, C., & Gao, Y. (2014). Uncovering Patterns of Inter-Urban Trip and Spatial Interaction from Social Media Check-In Data. *PLOS ONE*, *9*(1), e86026. 39. https://doi.org/10.1371/journal.pone.0086026

Louail, T., Lenormand, M., Picornell, M., García Cantú, O., Herranz, R., Frias-Martinez, E., Ramasco, J. J., & Barthelemy, M. (2015). Uncovering the spatial structure of mobility networks. *Nature Communications*, *6*, 6007. 83. https://doi.org/10.1038/ncomms7007

Maeda, T. N., Shiode, N., Zhong, C., Mori, J., & Sakimoto, T. (2019). Detecting and understanding urban changes through decomposing the numbers of visitors' arrivals using human mobility data. *Journal of Big Data*, *6*(1), 4. https://doi.org/10.1186/s40537-019-0168-5

Mieszkowski, P., & Mills, E. S. (1993). The Causes of Metropolitan Suburbanization. *Journal of Economic Perspectives*, *7*(3), 135–147. https://doi.org/10.1257/jep.7.3.135

Newman, M. (2010). *Networks: An Introduction* (1st Edition). Oxford University Press.

Noulas, A., Scellato, S., Lathia, N., & Mascolo, C. (2012). Mining User Mobility Features for Next Place Prediction in Location-Based Services. *2012 IEEE 12th International Conference on Data Mining (ICDM)*, 1038–1043. https://doi.org/10.1109/ICDM.2012.113

Opsahl, T., & Panzarasa, P. (2009). Clustering in weighted networks. *Social Networks*, *31*(2), 155–163. https://doi.org/10.1016/j.socnet.2009.02.002

Pan, J., & Lai, J. (2019). Spatial pattern of population mobility among cities in China: Case study of the National Day plus Mid-Autumn Festival based on Tencent migration data. *Cities*, *94*, 55–69. https://doi.org/10.1016/j.cities.2019.05.022

Parthasarathi, P. (2014). Network structure and metropolitan mobility. *Journal of Transport and Land Use*, *7*(2), 153. https://doi.org/10.5198/jtlu.v7i2.494

Partridge, M. D., & Rickman, D. S. (2008). Distance from Urban Agglomeration Economies and Rural Poverty. *Journal of Regional Science*, *48*(2), 285–310. https://doi.org/10.1111/j.1467-9787.2008.00552.x

Pinho, P., Silva, C., & Silva, C. (2016). *Mobility Patterns and Urban Structure*. Routledge. https://doi.org/10.4324/9781315595771

Puura, A., Silm, S., & Ahas, R. (2018). The Relationship between Social Networks and Spatial Mobility: A Mobile-Phone-Based Study in Estonia. *Journal of Urban Technology*, *25*(2), 7–25. https://doi.org/10.1080/10630732.2017.1406253

Ratti, C., Pulselli, R. M., Williams, S., & Frenchman, D. (2006). Mobile Landscapes: Using location data from cell phones for urban analysis. *Environment and Planning B: Planning and Design*, *33*(5), 727–748. 47. https://doi.org/10.1068/b32047

Ratti, C., Sobolevsky, S., Calabrese, F., Andris, C., Reades, J., Martino, M., Claxton, R., & Strogatz, S. H. (2010). Redrawing the Map of Great Britain from a Network of Human Interactions. *PLOS ONE*, *5*(12), e14248. https://doi.org/10.1371/journal.pone.0014248

Ravasz, E., & Barabási, A.-L. (2003). Hierarchical organization in complex networks. *Physical Review E*, *67*(2), 026112. https://doi.org/10.1103/PhysRevE.67.026112

Riascos, A. P., & Mateos, J. L. (2020). Networks and long-range mobility in cities: A study of more than one billion taxi trips in New York City. *Scientific Reports*, *10*(1), 1–14. https://doi.org/10.1038/s41598-020-60875-w

Roth, C., Kang, S. M., Batty, M., & Barthélemy, M. (2011). Structure of Urban Movements: Polycentric Activity and Entangled Hierarchical Flows. *PLOS ONE*, *6*(1), e15923. https://doi.org/10.1371/journal.pone.0015923

Saberi, M., Mahmassani, H. S., Brockmann, D., & Hosseini, A. (2017). A complex network perspective for characterizing urban travel demand patterns: Graph theoretical analysis of large-scale origin–destination demand networks. *Transportation*, *44*(6), 1383–1402. https://doi.org/10.1007/s11116-016-9706-6

Shaw, S.-L., Tsou, M.-H., & Ye, X. (2016). Editorial: Human dynamics in the mobile and big data era. *International Journal of Geographical Information Science*, *30*(9), 1687–1693. https://doi.org/10.1080/13658816.2016.1164317

Shen, J., & Cheng, T. (2016). A framework for identifying activity groups from individual space-time profiles. *International Journal of Geographical Information Science*, *30*(9), 1785–1805. https://doi.org/10.1080/13658816.2016.1139119

Shenzhen Municipal Statistics Bureau. (2016). *Shenzhen Statistical Yearbook 2016*. China Statistics Press. http://www.sz.gov.cn/cn/xxgk/zfxxgj/tjsj/tjnj/201701/W020170120506125327799.pdf.http://www.sz.gov.cn/cn/xxgk/zfxxgj/tjsj/tjnj/201701/W020170120506125327799.pdf

Simini, F., González, M. C., Maritan, A., & Barabási, A.-L. (2012). A universal model for mobility and migration patterns. *Nature*, *484*(7392), 96–100. https://doi.org/10.1038/nature10856

Song, C., Koren, T., Wang, P., & Barabási, A.-L. (2010). Modelling the scaling properties of human mobility. *Nature Physics*, *6*(10), 818–823. 80. https://doi.org/10.1038/nphys1760

Song, C., Qu, Z., Blumm, N., & Barabási, A.-L. (2010). Limits of Predictability in Human Mobility. *Science*, *327*(5968), 1018–1021. 2. https://doi.org/10.1126/science.1177170

Sun, L., Jin, J. G., Axhausen, K. W., Lee, D.-H., & Cebrian, M. (2015). Quantifying long-term evolution of intra-urban spatial interactions. *Journal of The Royal Society Interface*, *12*(102), 20141089. https://doi.org/10.1098/rsif.2014.1089

Tachet, R., Sagarra, O., Santi, P., Resta, G., Szell, M., Strogatz, S. H., & Ratti, C. (2017). Scaling Law of Urban Ride Sharing. *Scientific Reports*, *7*, 42868. https://doi.org/10.1038/srep42868

Tang, J., Liu, F., Wang, Y., & Wang, H. (2015). Uncovering urban human mobility from large scale taxi GPS data. *Physica A: Statistical Mechanics and Its Applications*, *438*, 140–153. https://doi.org/10.1016/j.physa.2015.06.032

Toole, J. L., Herrera-Yaqüe, C., Schneider, C. M., & González, M. C. (2015). Coupling human mobility and social ties. *Journal of The Royal Society Interface*, *12*(105), 20141128. https://doi.org/10.1098/rsif.2014.1128

Tu, W., Cao, J., Yue, Y., Shaw, S.-L., Zhou, M., Wang, Z., Chang, X., Xu, Y., & Li, Q. (2017). Coupling mobile phone and social media data: A new approach to understanding urban functions and diurnal patterns. *International Journal of Geographical Information Science*, *31*(12), 2331–2358. https://doi.org/10.1080/13658816.2017.1356464

Tu, W., Cao, R., Yue, Y., Zhou, B., Li, Q., & Li, Q. (2018). Spatial variations in urban public ridership derived from GPS trajectories and smart card data. *Journal of Transport Geography*, *69*, 45–57. https://doi.org/10.1016/j.jtrangeo.2018.04.013

Tu, W., Santi, P., Zhao, T., He, X., Li, Q., Dong, L., Wallington, T. J., & Ratti, C. (2019). Acceptability, energy consumption, and costs of electric vehicle for ride-hailing drivers in Beijing. *Applied Energy*, *250*, 147–160. https://doi.org/10.1016/j.apenergy.2019.04.157

Wang, P., Fu, Y., Zhang, J., Li, X., & Lin, D. (2018). Learning Urban Community Structures: A Collective Embedding Perspective with Periodic Spatial-temporal Mobility Graphs. *ACM Transactions on Intelligent Systems and Technology*, *9*(6), 63:1–63:28. https://doi.org/10.1145/3209686

Wang, X.-W., Han, X.-P., & Wang, B.-H. (2014). Correlations and Scaling Laws in Human Mobility. *PLOS ONE*, *9*(1), e84954. https://doi.org/10.1371/journal.pone.0084954

Wang, Y., Wang, F., Zhang, Y., & Liu, Y. (2019). Delineating urbanization “source-sink” regions in China: Evidence from mobile app data. *Cities*, *86*, 167–177. https://doi.org/10.1016/j.cities.2018.09.016

Watts, D. J., & Strogatz, S. H. (1998). Collective dynamics of ‘small-world’ networks. *Nature*, *393*(6684), 440. https://doi.org/10.1038/30918

Wu, L., & Zhang, J. (2011). Accelerating growth and size-dependent distribution of human online activities. *Physical Review E*, *84*(2). https://doi.org/10.1103/PhysRevE.84.026113

Wu, L., Zhi, Y., Sui, Z., & Liu, Y. (2014). Intra-Urban Human Mobility and Activity Transition: Evidence from Social Media Check-In Data. *PLOS ONE*, *9*(5), e97010. 35. https://doi.org/10.1371/journal.pone.0097010

Xu, Y., Chen, D., Zhang, X., Tu, W., Chen, Y., Shen, Y., & Ratti, C. (2019). Unravel the landscape and pulses of cycling activities from a dockless bike-sharing system. *Computers, Environment and Urban Systems*, *75*, 184–203. https://doi.org/10.1016/j.compenvurbsys.2019.02.002

Xu, Y., Shaw, S.-L., Zhao, Z., Yin, L., Fang, Z., & Li, Q. (2015). Understanding aggregate human mobility patterns using passive mobile phone location data: A home-based approach. *Transportation*, *42*(4), 625–646. https://doi.org/10.1007/s11116-015-9597-y

Xu, Y., Shaw, S.-L., Zhao, Z., Yin, L., Lu, F., Chen, J., Fang, Z., & Li, Q. (2016). Another Tale of Two Cities: Understanding Human Activity Space Using Actively Tracked Cellphone Location Data. *Annals of the American Association of Geographers*, *106*(2), 489–502. https://doi.org/10.1080/00045608.2015.1120147

Yan, X.-Y., Han, X.-P., Wang, B.-H., & Zhou, T. (2013). Diversity of individual mobility patterns and emergence of aggregated scaling laws. *Scientific Reports*, *3*, 2678. 79. https://doi.org/10.1038/srep02678

Yang, X., Fang, Z., Xu, Y., Yin, L., Li, J., & Lu, S. (2019). Spatial heterogeneity in spatial interaction of human movements—Insights from large-scale mobile positioning data. *Journal of Transport Geography*, *78*, 29–40. https://doi.org/10.1016/j.jtrangeo.2019.05.010

Yang, X., Fang, Z., Yin, L., Li, J., Lu, S., & Zhao, Z. (2019). Revealing the relationship of human convergence–divergence patterns and land use: A case study on Shenzhen City, China. *Cities*, *95*, 102384. https://doi.org/10.1016/j.cities.2019.06.015

Yildirimoglu, M., & Kim, J. (2017). Identification of communities in urban mobility networks using multi-layer graphs of network traffic. *Transportation Research Procedia*, *27*, 1034–1041. https://doi.org/10.1016/j.trpro.2017.12.070

Zeng, A., Shen, Z., Zhou, J., Wu, J., Fan, Y., Wang, Y., & Stanley, H. E. (2017). The science of science: From the perspective of complex systems. *Physics Reports*, *714–715*, 1–73. https://doi.org/10.1016/j.physrep.2017.10.001

Zhang, S., Tang, J., Wang, H., Wang, Y., & An, S. (2017). Revealing intra-urban travel patterns and service ranges from taxi trajectories. *Journal of Transport Geography*, *61*, 72–86. https://doi.org/10.1016/j.jtrangeo.2017.04.009

Zhang, W., & Thill, J.-C. (2017). Detecting and visualizing cohesive activity-travel patterns: A network analysis approach. *Computers, Environment and Urban Systems*, *66*, 117–129. https://doi.org/10.1016/j.compenvurbsys.2017.08.004

Zhang, X., Xu, Y., Tu, W., & Ratti, C. (2018). Do different datasets tell the same story about urban mobility—A comparative study of public transit and taxi usage. *Journal of Transport Geography*, *70*, 78–90. https://doi.org/10.1016/j.jtrangeo.2018.05.002

Zhao, Y., Zhang, H., An, L., & Liu, Q. (2018). Improving the approaches of traffic demand forecasting in the big data era. *Cities*, *82*, 19–26. https://doi.org/10.1016/j.cities.2018.04.015

Zheng, Z., & Zhou, S. (2017). Scaling laws of spatial visitation frequency: Applications for trip frequency prediction. *Computers, Environment and Urban Systems*, *64*, 332–343. 82. https://doi.org/10.1016/j.compenvurbsys.2017.04.004

Zhong, C., Schläpfer, M., Arisona, S. M., Batty, M., Ratti, C., & Schmitt, G. (2015). Revealing centrality in the spatial structure of cities from human activity patterns. *Urban Studies*, 0042098015601599. https://doi.org/10.1177/0042098015601599